

第五章 量子微纳光学

5.1 分子荧光

5.2 纳米结构近场区域偶极子弛豫系数

5.3 SPP增强分子荧光的前沿进展

5.4 SPP 的量子性

5.5 基于超表面的量子性质

5.6 基于拓扑光子结构的量子性质

5.7 微纳尺度腔量子电动力学及应用

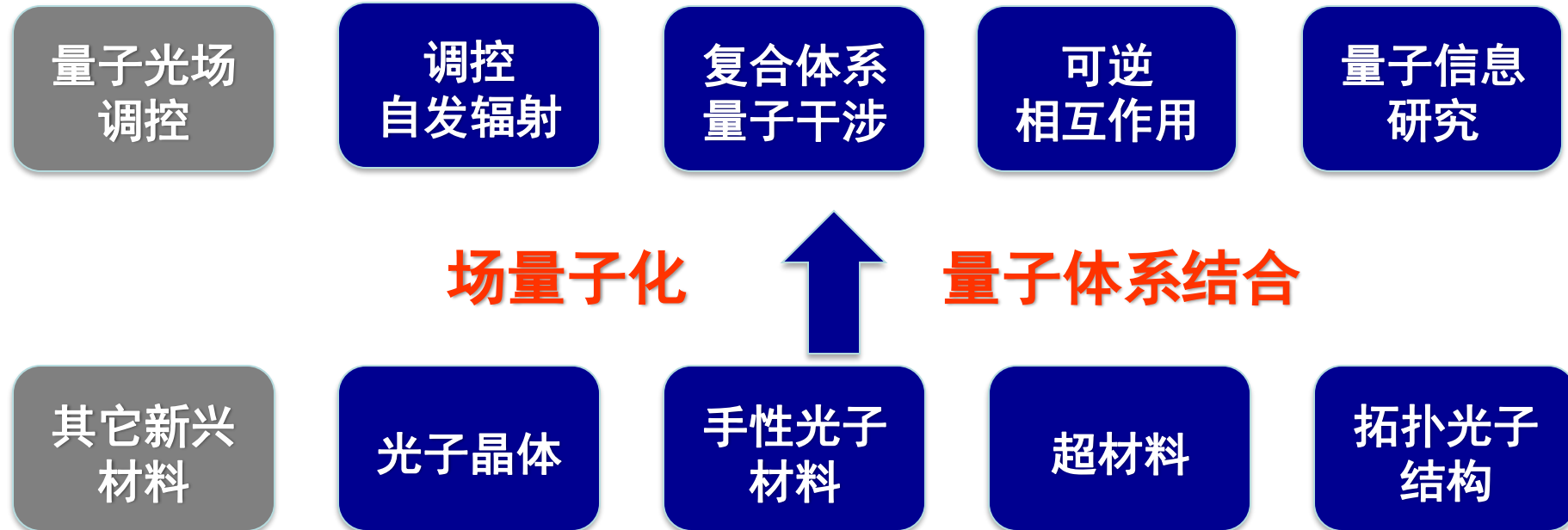
5.7 微纳尺度腔量子电动力学及应用

腔量子电动力学

Cavity Quantum ElectroDynamics
CQED



纳米或亚波长尺度



- 解析求解表面等离激元的方法及应用
- 基于表面等离激元光学的CQED及应用
- 基于复合纳米结构的CQED

表面等离激元：解析求解本征模式的研究方法

任何表面等离激元激发
可以看做各种电磁波本
征模式的叠加

$$\Psi = \sum P_i \Phi_i$$

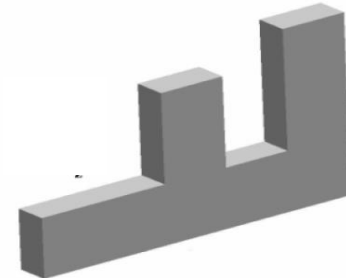
本征模式是分析表面等离激
元传播、局域、调控及应用
的基础

只有简单的或对称性高的纳米结构的本征模式才能解
析给出，其它情况只能用数值模拟软件

我们发展的格林矩阵等方法
能够解析给出不规则结构和多层膜等的本征模式

我们的格林矩阵方法

解决不规则纳米颗粒结构的局域模式



本征问题：由纳米金属颗粒几何形状决定的格林并矢矩阵

本征值 \leftrightarrow **本征材料参数**

本征矢 \leftrightarrow **给出近场分布**

$$G^0(\mathbf{r}, \mathbf{r}', \omega) = \left(\mathbf{I} - \frac{1 - ik_0 R}{k_0^2 R^2} \mathbf{I} - \frac{-3 + 3ik_0 R + k_0^2 R^2}{k_0^2 R^4} \mathbf{R} \mathbf{R} \right) \frac{\exp[ik_0 R]}{4\pi R}$$

$$\tilde{\vec{E}}(\mathbf{r}) = \sum_{n=1}^{3N} \frac{s \mathbf{L}_n \cdot \widetilde{\vec{E}^0}(\mathbf{r})}{(s - s_n)} \cdot \mathbf{R}_n$$

$$\epsilon_n = \frac{1}{s_n} + \epsilon_0(\omega)$$

从而可以设计和裁剪局域表面等离激元

PRB (2003, 2004(3))

EPL (2008)

Appl Phys B (2010)

J Appl Phys (2010) 等

传播表面等离激元：解析求解传播本征模式的研究方法

表面等离激元波导

缺点：传播长度短、被被动调谐

策略：加入纳米介质层和液晶等

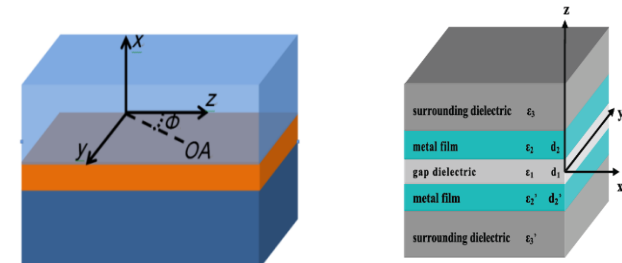
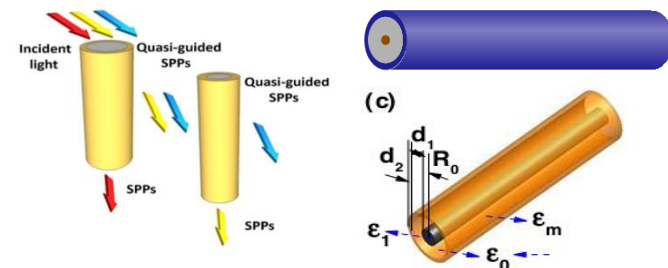
解析求解多层柱状和薄膜波导模式

通过模式分析：

亚波长光限制和长程传播传播的杂化模式、可主动调谐的波导模式

分束器、干涉仪等纳米光子器件

信息传输速度快、实现器件的小型化



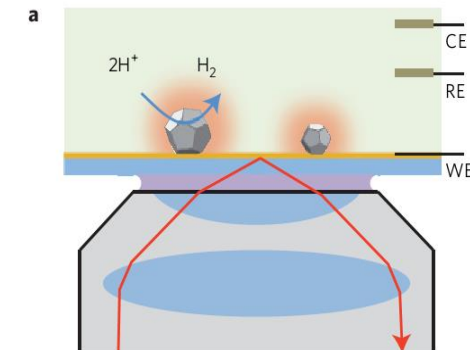
Appl Phys Lett (2013)
Opt Lett (2014)
Plasmonics (2013)
Appl Phys B (2011) 等

解析求解本征模式的研究方法

局域模式的格林矩阵方法
传播模式的解析方法 } 两者互补

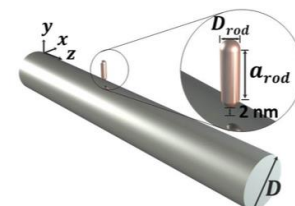
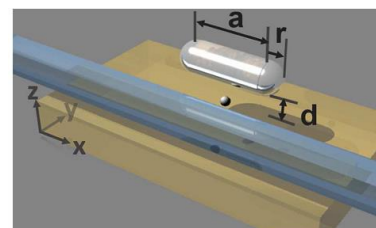
表面等离激元模式分析：

局域模式+传播模式+耦合或叠加



Nat. Nanotech. (2012)

为我们后面在量子表面等离激
元及其它领域应用提供积累和
准备



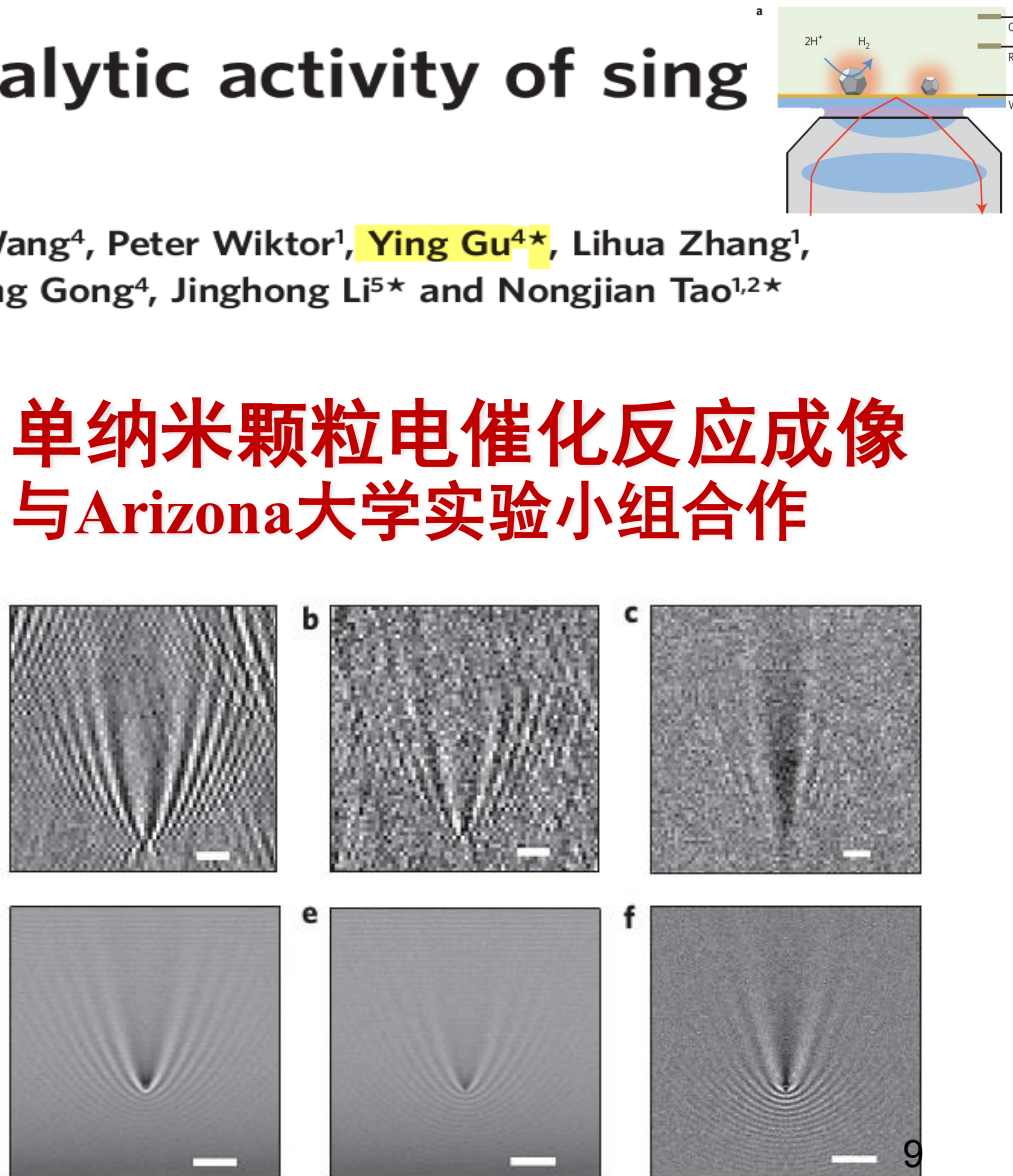
Phys. Rev. Lett.
(2015, 2017, 2021)

Imaging the electrocatalytic activity of single nanoparticles

Xiaonan Shan^{1,2}, Ismael Díez-Pérez^{1,3}, Luojia Wang⁴, Peter Wiktor¹, Ying Gu^{4*}, Lihua Zhang¹, Wei Wang¹, Jin Lu^{1,5}, Shaopeng Wang¹, Qihuang Gong⁴, Jinghong Li^{5*} and Nongjian Tao^{1,2*}

理论上的重要贡献
三位共同通讯作者之一

系统模拟了纳米颗粒在表面等离激元波的散射中的近场图样，利用局域场效应清楚地揭示了电催化反应成像的物理机制

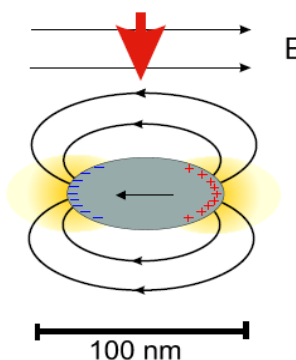
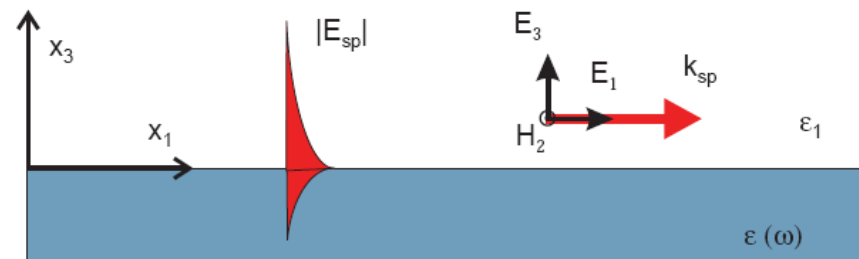
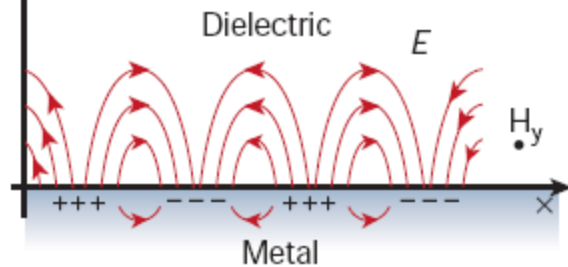


- 解析求解表面等离激元的方法及应用
- 基于表面等离激元光学的CQED及应用
- 基于复合纳米结构的CQED

表面等离激元 (SPP)

a

SPP: 自由电子的集体震荡
倏逝的电磁模式束缚在界面



局域SP或SPR:
局域振荡
强局域场

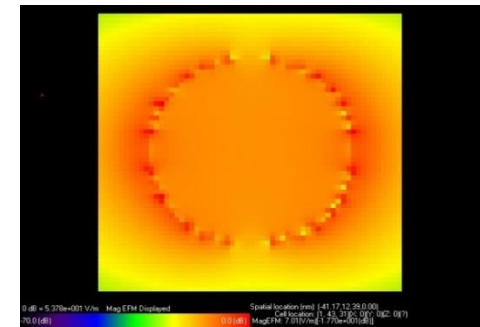
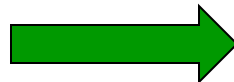
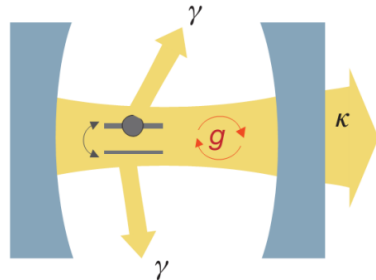


Figure 1.3: Particle plasmon



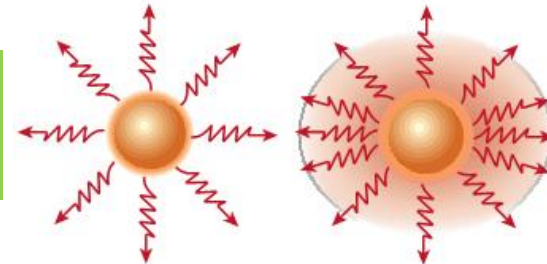
亚波长的局域场效应 (超小的模式体积)

局域场效应，为光与量子体系相互作用 带来什么新的研究机会？



Weak Coupling $g \ll \gamma, \kappa$

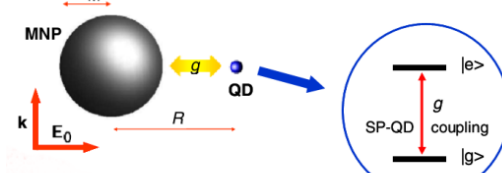
Purcell 效应



g Coupling strength
 γ damping of emitter
 κ damping of cavity

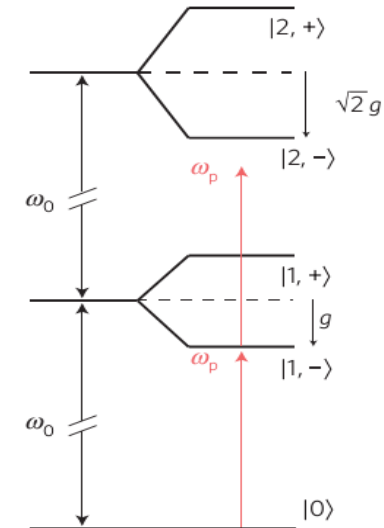
Moderate coupling

$$\gamma_{QD} < g < \kappa_{sp}$$



Strong Coupling
 $g \gg \gamma, \kappa$

Rabi劈裂



Nature 480,193(2011); Nature 424,839(2003); Nphy 9,329(2013)

在弱耦合区域，有什么结果？

量子发射体的弛豫速率调节

$$\Gamma = \frac{2}{\hbar} \operatorname{Im}\{\mu_i G_{ij}(0, \omega_A) \mu_j\}$$

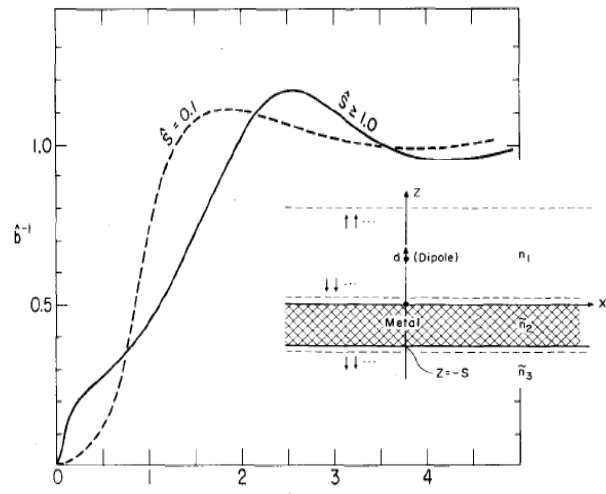
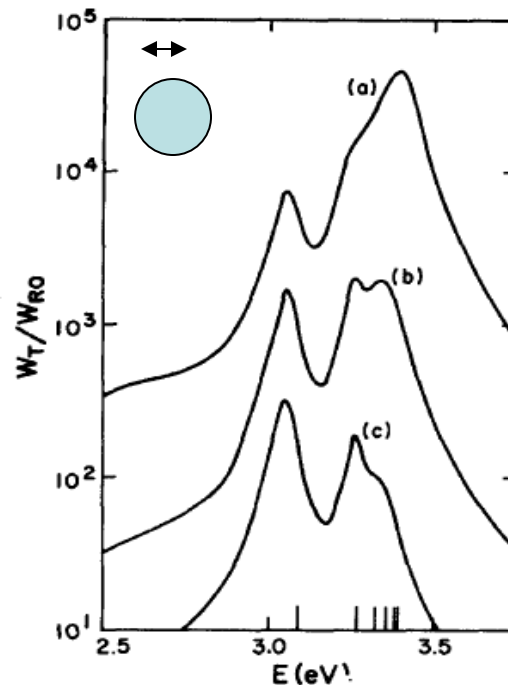


FIG. 5. The effect of the thickness of the metal mirror on the



表面等离基元的特点：

1. 大的Purcell系数
2. 各向异性弛豫速率

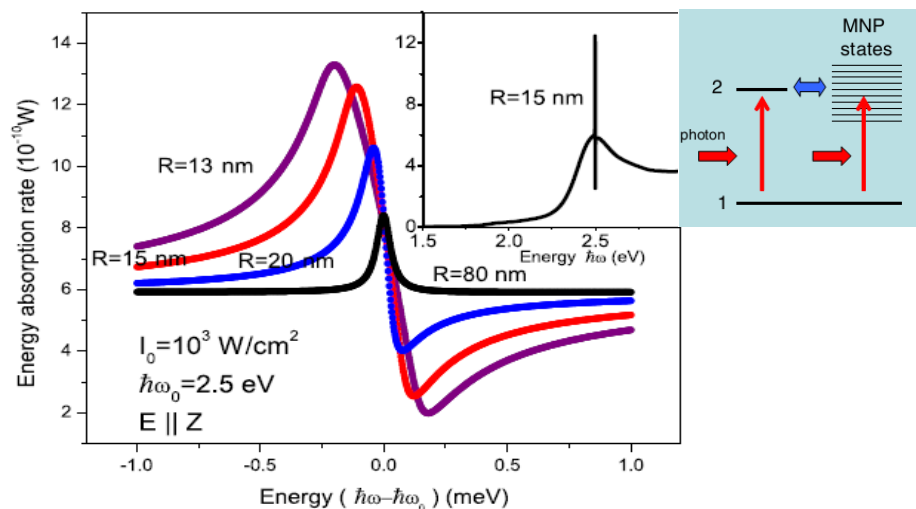
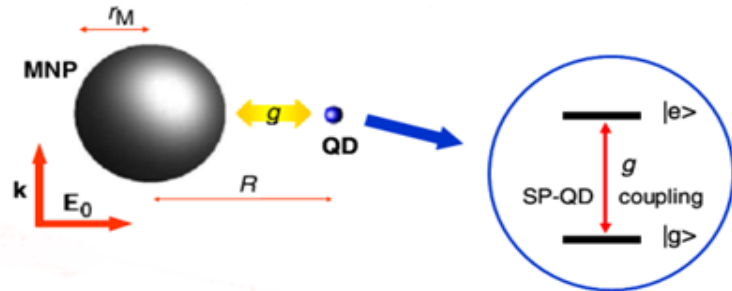
R.R.Chance et al, the journal of chemical physics, 62,2245 (1975); R. Rupp, J. Chem.Phys. 76,1681 (1982).

在中等耦合区域,有什么结果?

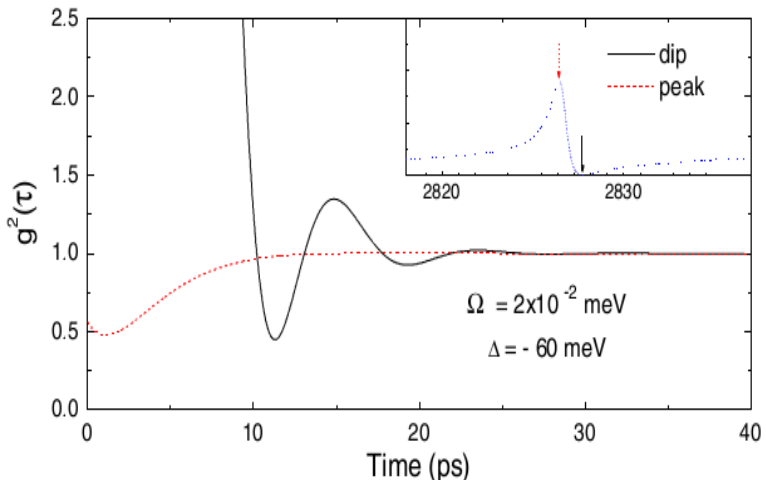
QD哈密顿量
相互作用过程

反馈机制

$$H = \hbar\omega_e \sigma_{ee} + \hbar\omega_g \sigma_{gg} - \mu_{eg} (\sigma_{eg} + \sigma_{ge}) E_{QD}$$

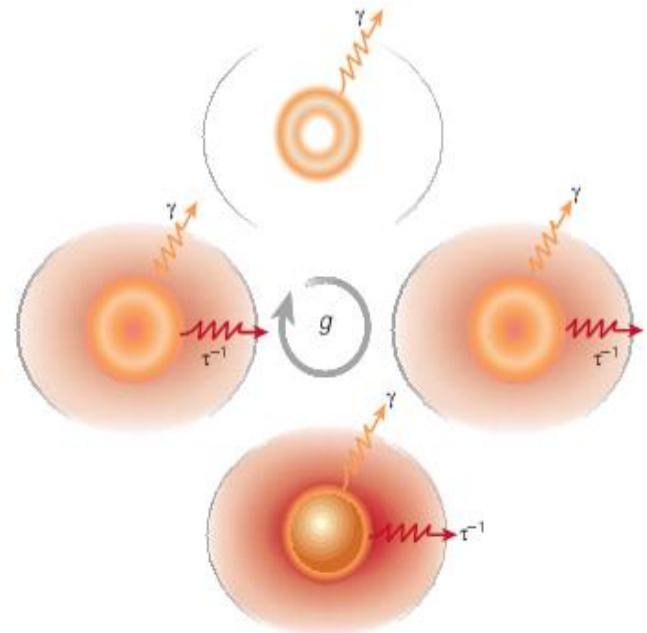


Fano线型, 吸收的展宽和红移



单光子性

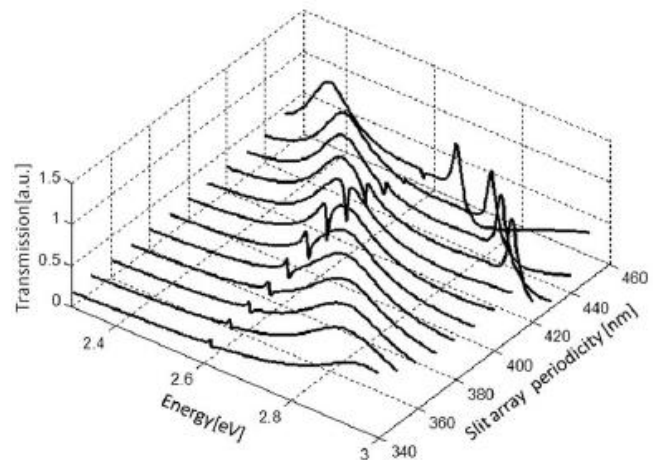
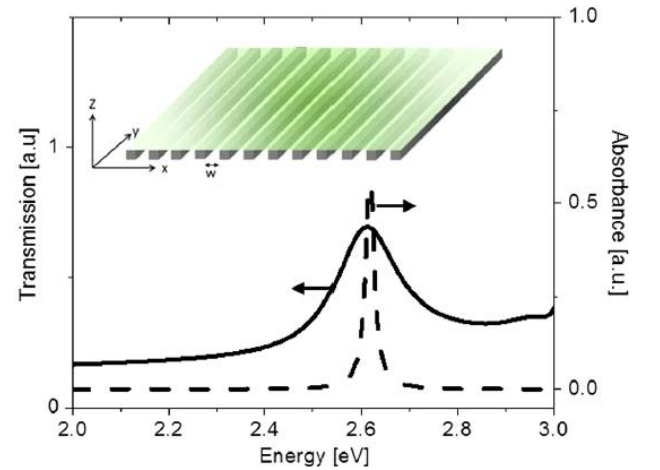
在强耦合区域,有什么结果?



由于:

1. 强近场增强
2. 压缩的局部场分布

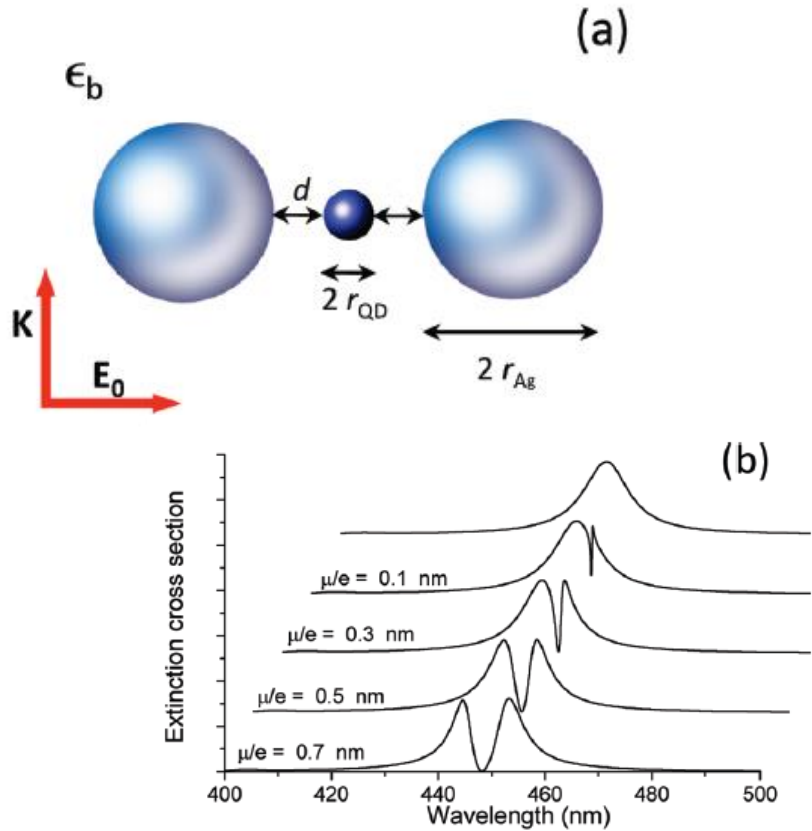
将不可逆的自发辐射过程转换为emitter和腔模可逆的能量交换过程



SPP的Rabi劈裂

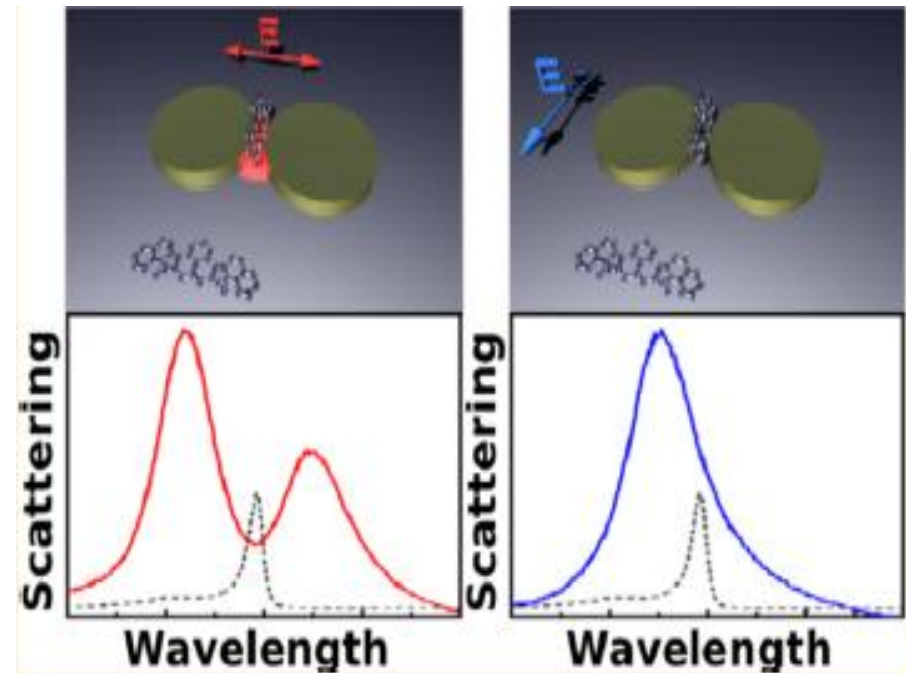
强耦合的其他主要进展

-----单独结构的强耦合



理论上证明了金属小球
二聚物的强耦合

ACSNano4, 6369(2010)



首先观察到表面等离激元二聚物的强耦合

Nano Letters. 13, 3281–3286(2013)

- 弱耦合范畴
 - 高效可调方向性单光子发射
 - 各向异性珀赛尔系数调控量子相干性质
- 中等耦合范畴
 - 借助于表面等离激元的无粒子数反转增益
- 强耦合范畴
 - 條逝波下的耦合因子增强

提出纳米尺度导引的高效单光子发射

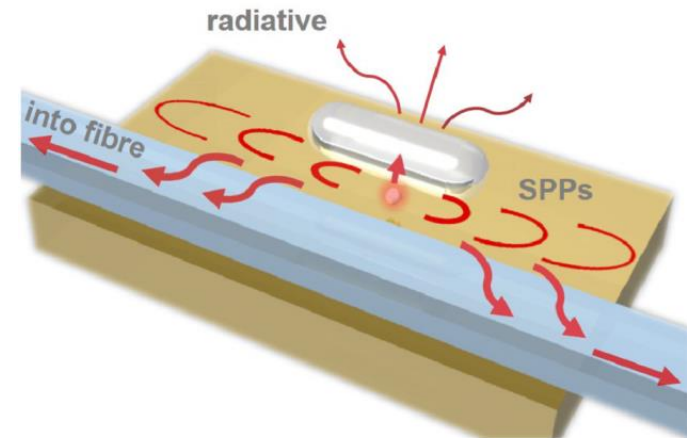
纳米尺度单光子源是实现芯片上量子信息处理的瓶颈问题之一

存在的问题：

介质中单光子发射率低

(真空中的几十倍)

金属中单光子发射率高但损耗大



我们的解决方案

提出金属和光纤复合纳米结构，

达到同时高效产生和收集单光子的目的

Y. Gu et al.
Phys. Rev. Lett. (2015)

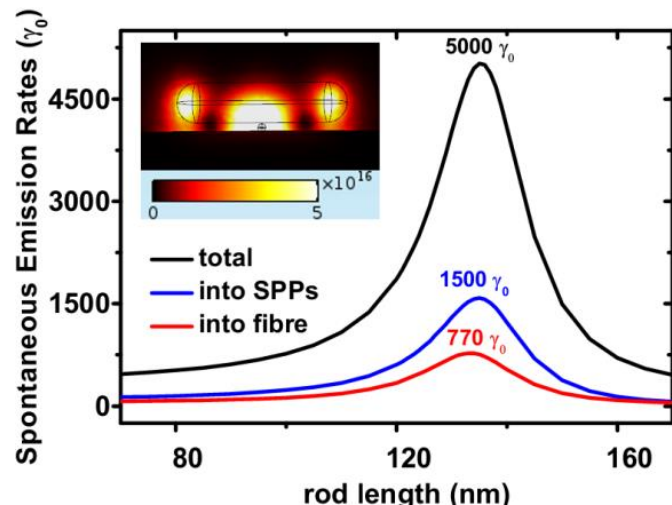
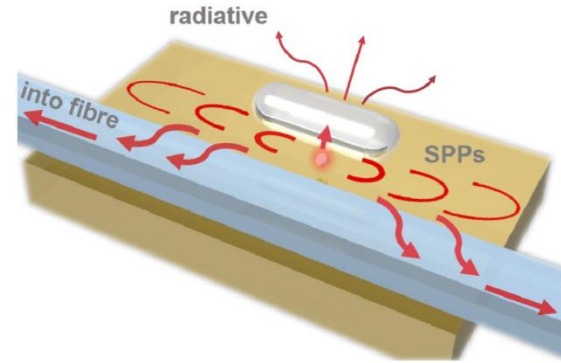
结合两者优势：

间隙表面等离激元超高的单光子发射率，低损耗纳米光纤高效提取单光子的传播部分

达到：

直接由纳米光纤通道提取单光子发射率可达真空中的700倍

有望用于芯片上亮单光子源



Hang Lian, Ying Gu*, Juanjuan Ren, Fan Zhang, Luojia Wang, and Qihuang Gong, [Efficient Single Photon Emission and Collection Based on Excitation of Gap Surface Plasmons](#)
PHYSICAL REVIEW LETTERS 114, 193002 (2015).

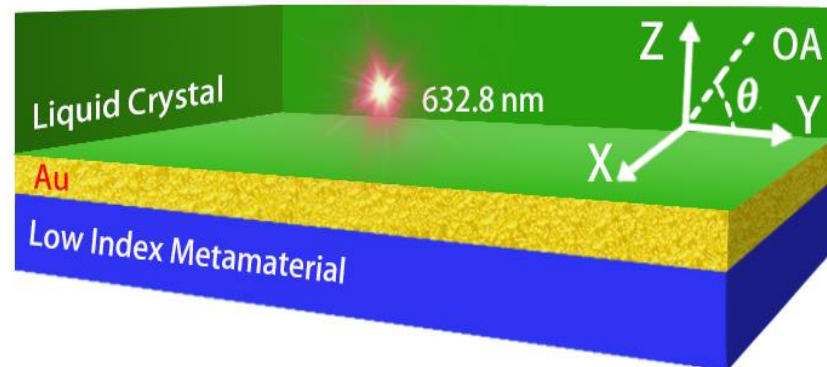
提出微纳尺度上主动式的自发辐射调控方案

主动式的自发辐射调控是限制可调谐的纳米光学器件的关键

现有的被动式调节：

改变几何尺寸

(不灵活， 不可连续调节)



我们的解决方案：

提出液晶，金属，低折射率超材料的复合纳米等离激元结构，实现主动，连续，可逆，宽带的自发辐射调控

结合两者优势：

液晶：主动调控

低折射率超材料：增强自发辐射

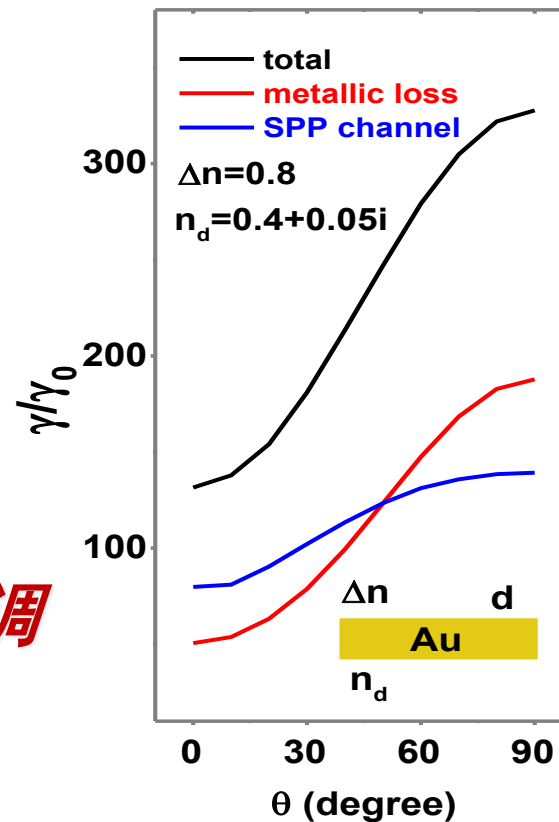
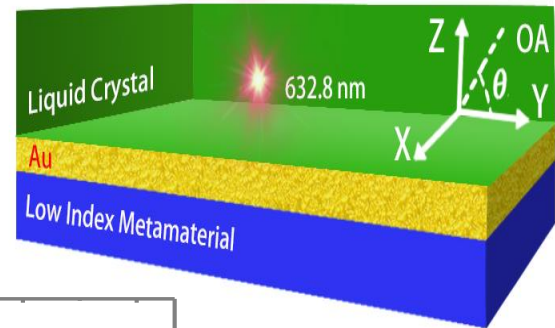
实现了：

自发辐射速率从 $131 \gamma_{\text{J0}}$
到 $327 \gamma_{\text{J0}}$ 的主动调控

调节有效波长范围

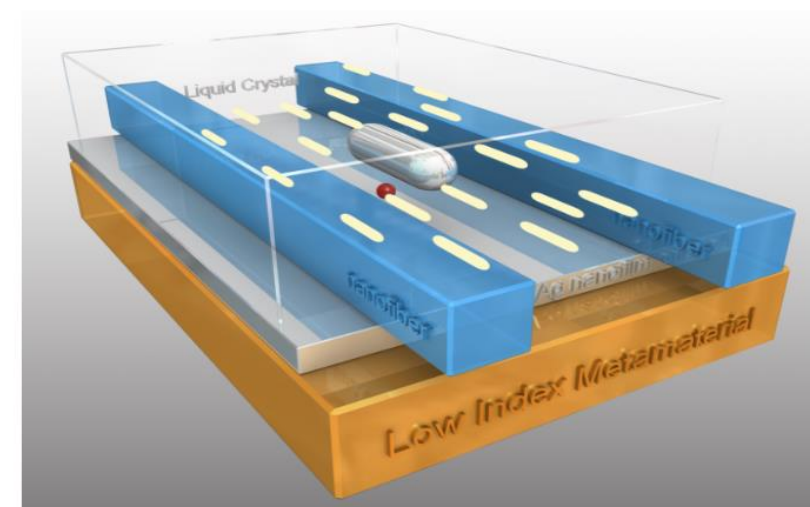
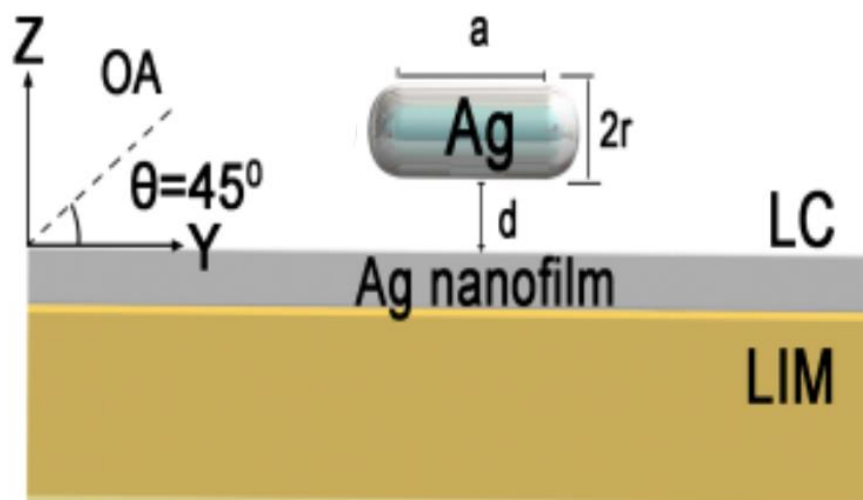
550 nm —— 800 nm

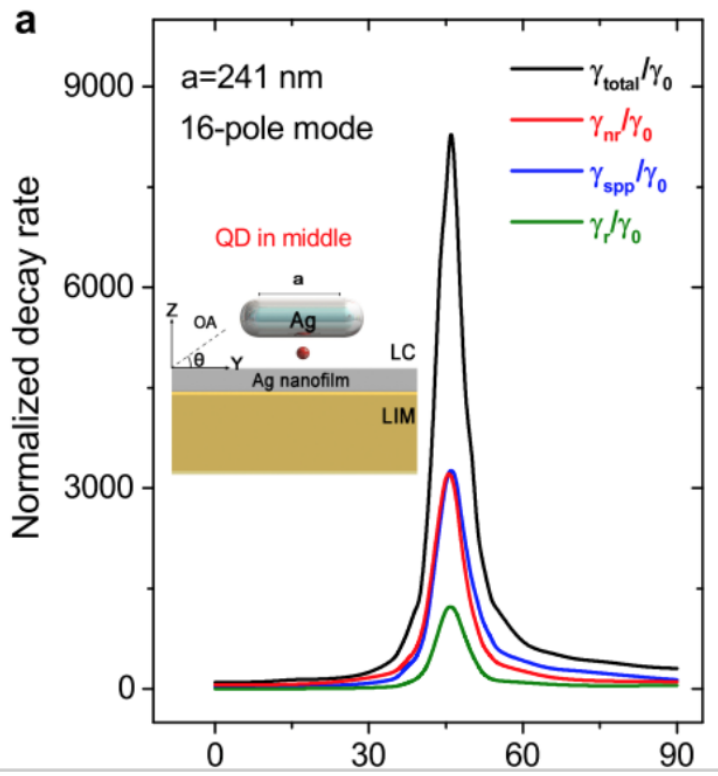
可用于调控单光子源，调
控激光阈值



High contrast switching and high-efficiency routing of spontaneous emission

Gap surface plasmon → more localized field → more enhanced spontaneous emission





$$\gamma_{\text{total}} = \gamma_{\text{SPP}} + \gamma_{\text{nr}} + \gamma_r$$

$\gamma_{\text{total}} \quad 103 \gamma_0 \sim 8750 \gamma_0 \quad \text{c=85}$

$\gamma_{\text{spp}} \quad 42 \gamma_0 \sim 3726 \gamma_0$

$\gamma_{\text{nr}} \quad 60 \gamma_0 \sim 3643 \gamma_0$

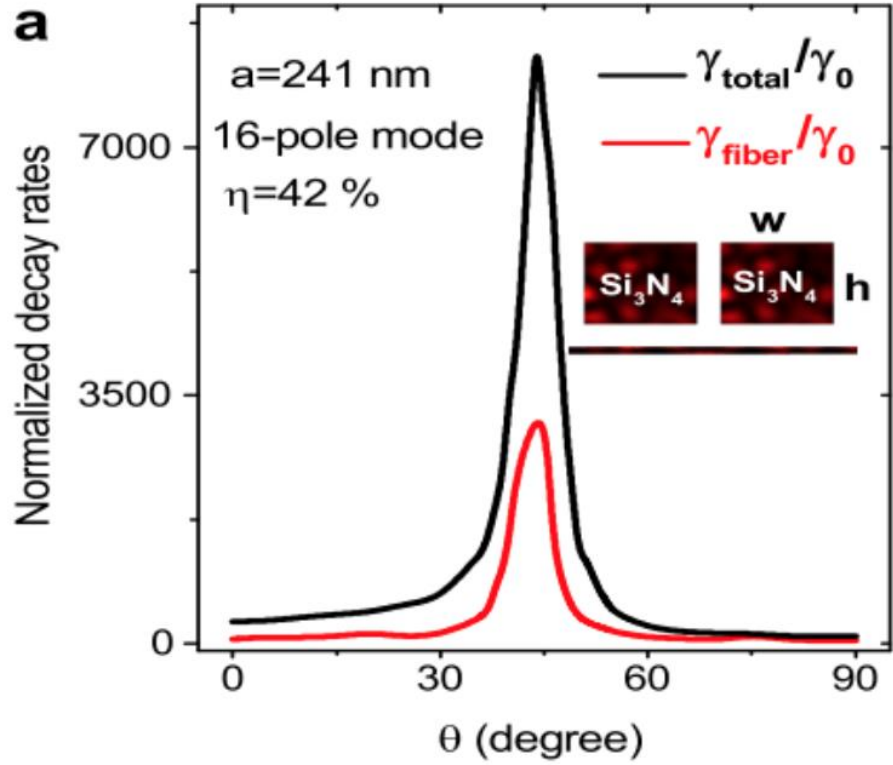
$\gamma_r \quad \gamma_0 \sim 1381 \gamma_0$

Contrast ratio C = $\gamma_{\text{max}}/\gamma_{\text{min}}$

$35^\circ \sim 45^\circ$

$C=10$

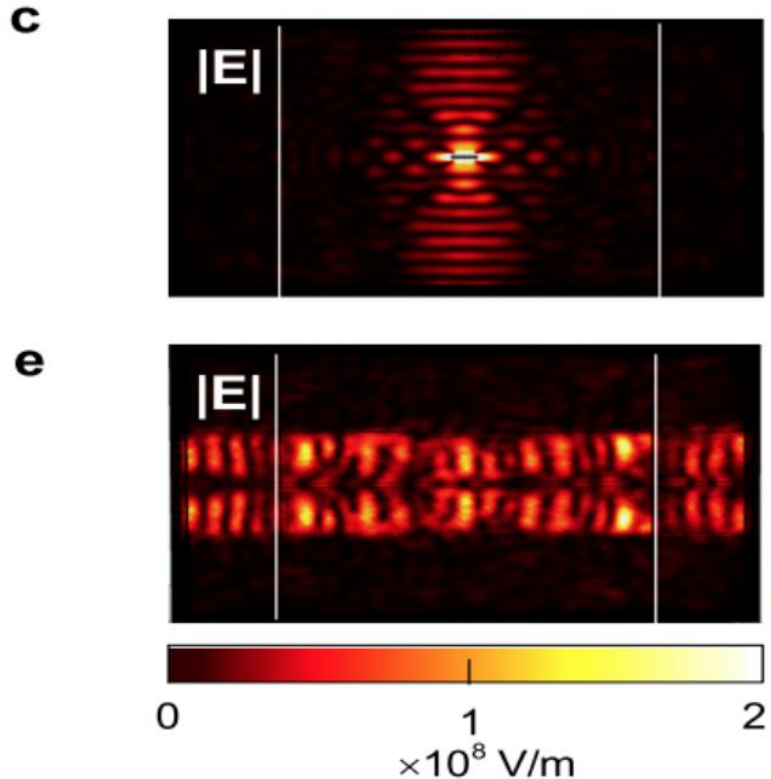
Fast response time ns



$$\eta = \gamma_{\text{fiber}} / \gamma_{\text{total}}$$

collection efficiency

Up to 42% for 16-pole mode



利用表面等离激元的局域场效应及各向异性的珀塞爾系数，演示纳米尺度上的系列量子相干现象
例如：

单分子共振荧光

PRB(2010)

自发辐射谱线变窄

Nano Lett.(2012)

双囚禁电磁感应透明

Sci. Rep.(2013)

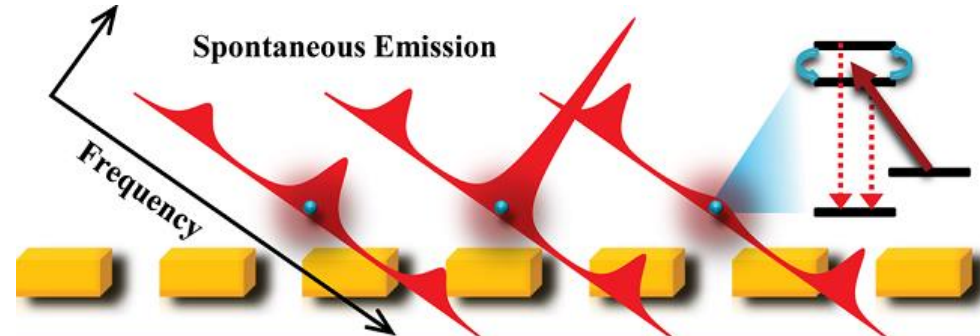
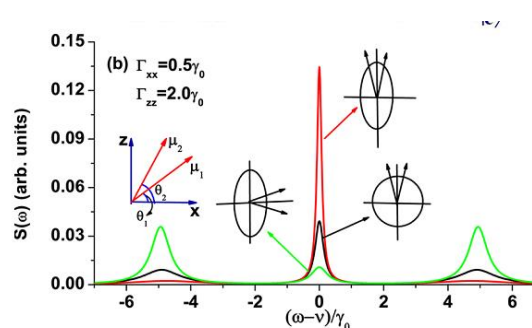
增强克尔非线性

Sci. Rep. (2015)

Surface-Plasmon-Induced Modification on the Spontaneous Emission Spectrum via Subwavelength-Confinement Anisotropic Purcell Factor

Ying Gu,^{*,†} Luojia Wang,[†] Pan Ren,[†] Junxiang Zhang,[‡] Tiancai Zhang,[‡] Olivier J. F. Martin,[§] and Qihuang Gong^{*,†}

控制机理：当两个偶极子的角平分线沿着有效弛豫系数椭球的长轴（短轴）时，消（增）相干导致中心谱线变窄（变宽）。



被Science、Nano Lett.、Acs nano、Adv. Opt. Mat.、Phys. Rev. Lett.、Opt. Lett.、Phys. Rev. A等引用超过半数实验文章，说明理论工作对实验的启发和促进

mechanism for a host of radiative and scattering processes associated with nanophotonic systems. Field enhancement has been shown to affect surface-enhanced Raman scattering (1); nonlinear processes, such as enhanced harmonic generation (2) or wave mixing (3); nanolasing (4); plasmonic sensing (5); and enhancement of spontaneous emission (6).

The largest field enhancements in nanoplasmonic systems occur near sharp asperities or corners associated with metal nanoparticles (NPs) and within the subnanometer gaps formed between NP aggregates. An incident optical field drives currents across the NP, resulting in peak currents flowing through the NP during

However, in a real metal, polarization charge densities are not perfectly localized at a surface but are slightly spread over a thickness near the boundary. This dispersion of the charge effectively removes the singularities: Charges no longer reside exactly at the surface, but acquire some volume as the charge density spreads into the NP. The scattering spectrum ceases to be continuous and is now discrete, with correspondingly reduced field enhancements (8, 9). These effects have long been recognized by theorists; for example, Fuchs and Sazanov (10) showed that the nonlocal effects considered here limit the response of almost-touching spheres.

The effect of including the pressure term in the electron response is that the longitudinal dielectric function, ϵ_L , becomes nonlocal, depending on the propagation vector \mathbf{k} in addition to the frequency, as follows:

$$\epsilon_L(\mathbf{k}, \omega) = 1 - \frac{\omega_p^2}{\omega^2 + i\gamma\omega - \beta^2|\mathbf{k}|^2} \quad (2)$$

whereas the transverse response is unchanged.

The simple picture, then, of a surface charge layer with infinitesimal extent must be replaced with a continuous charge density, whose extent

实验文章Science337, 1072 (2012) 将我们工作作为近场增益影响自发辐射的例子而引用

Surface charge density picture. Structures that possess a singularity, such as spheres that touch at a point, have been shown to possess continuous scattering spectra associated with compression of the surface plasmon wave field at the singularity. According to the local model, a pulse of surface plasmons launched into such a system

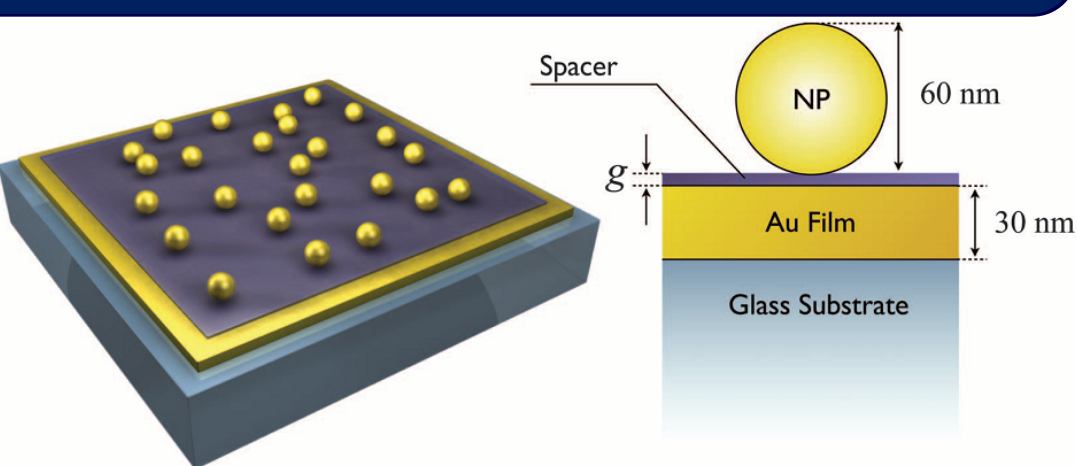


Fig. 1. Geometry of the film-coupled nanoparticle. (**Left**) Schematic of the sample. (**Right**) Cross section of a single film-coupled nanosphere.

¹Center for Metamaterials and Integrated Plasmonics and Department of Electrical and Computer Engineering, Duke University, Durham, NC 27708, USA. ²Center for Biologically Inspired Materials and Material Systems, Duke University, Durham, NC 27708, USA. ³Department of Physics, Blackett Laboratory, Imperial College London, London SW7 2AZ, UK. ⁴Department of Biomedical Engineering, Duke University, Durham, NC 27708, USA.

*To whom correspondence should be addressed. E-mail: cristian.ciraci@duke.edu

6 is due to the hybridization of the SQW exciton with LSP quadrupole modes. While there is now a rapidly growing literature demonstrating plasmon–exciton hybridization in heterostructures of Au nanoparticles and J-aggregate complexes or organic dyes,^{1–4,6,7} in addition to the impressive work demonstrating strong coupling between GaAs excitons and SPPs,⁵ this is the first demonstration of a hybridized LSP-

Liang, A.; Luo, T.; Du, G. *Chem. Phys. Lett.* **2008**, *400*, 340–351.

(12) Davis, J. A.; Dao, L. V.; Wen, X.; Ticknor, C.; Hannaford, P.; *Chem. Mater.* **2011**, *23*, 241–247.

states.^{1–5} The ability to control coherent interactions between nanoscale plasmonic and excitonic systems has opened up a wealth of possible applications for nanoquantum devices.^{6,7}

Grundmann, M. *Appl. Phys. A: Mater. Sci. Process.* **2007**, *88*, 99–104.

(14) Park, S.-H.; Ahn, D. *Appl. Phys. Lett.* **2005**, *87*, 253509.

6156

[dx.doi.org/10.1021/nl3029784](https://doi.org/10.1021/nl3029784) | *Nano Lett.* **2012**, *12*, 6152–6157

**4篇实验文章[Nano.Lett.、Acs Nano、Adv.Opt.Mat.、
Adv.Func.Mat.]中，作者多次提到这个工作并阐述了工作的意
义：认为对表面等离激元和激子之间相干相互作用的操控，开
启了纳米量子器件可能的应用，以及表面等离激元和激子的杂
化对量子体系光谱的精准调控是一个蓬勃发展的领域。**

tric environment (e.g., Purcell effect).⁹ This approach is becoming increasingly popular as methods to precisely control the relative position and orientation of active optical units at the nanoscale have become available.^{10,11} Interfaces,¹² microcavities,¹³ nanorods,^{14–18} nanospheres,^{19–25} gratings,²⁶ and photonic crystals²⁷ have been used to engineer the radiative emission rate and quantum efficiency of fluorophores.

plasmonic devices^{2,31} avoiding instability of the intermediates during the ligand exchange and assembly. Therefore additional methods are required to produce anisotropic emitter-plasmon nanostructures so as to forward the understanding of spacing, location, and dipole orientation on coupled plasmon–exciton photophysics.^{11,35,36,44} One critical factor limiting the high-yield low-variability

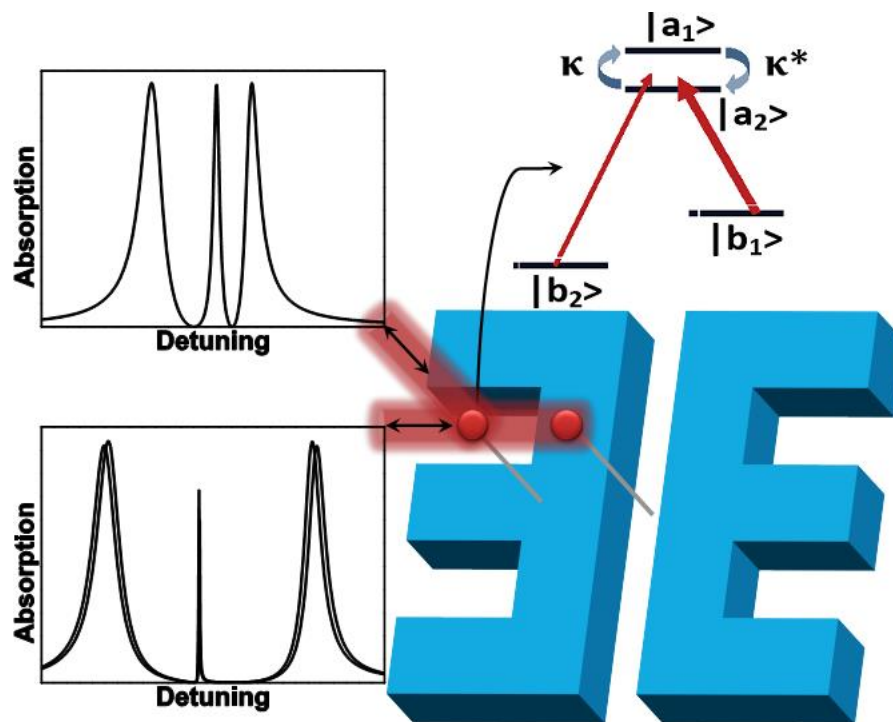
ce to

17, 2013
r 4, 2013.

mber 04, 2013

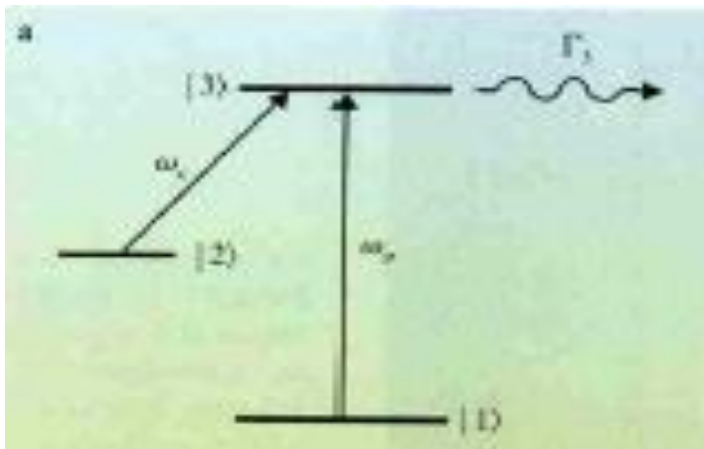
dipole field can be estimated with Fermi's © 2013 American Chemical Society

Polarized Linewidth-Controllable Double-Trapping EIT Spectra in a Resonant Plasmon Nanocavity



Luojia Wang, Ying Gu et al. Polarized linewidth-controllable double-trapping electromagnetically induced transparency spectra in a resonant plasmon nanocavity, Scientific Reports, 3, 2879 (2013).

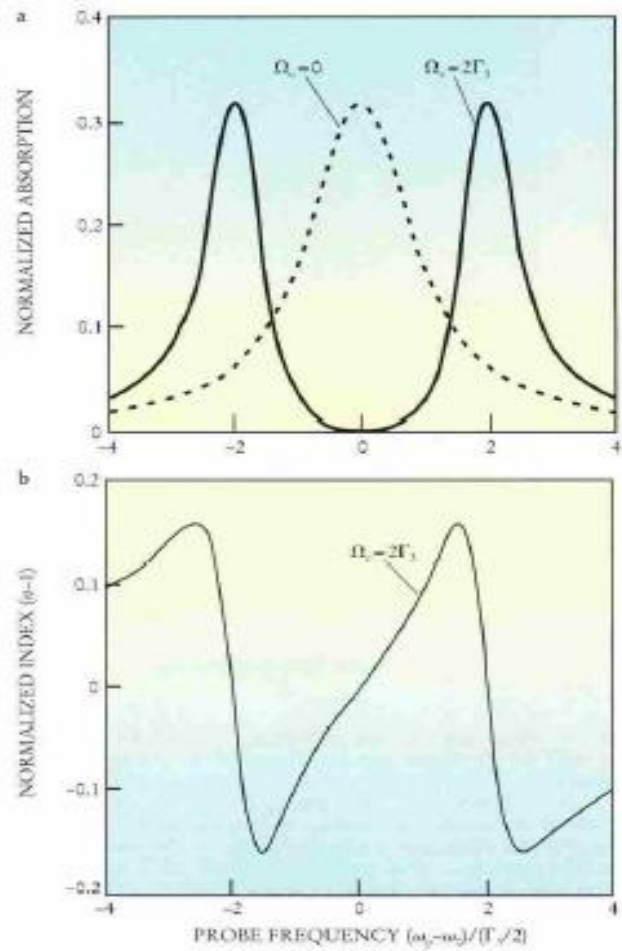
电磁感应透明(EIT)



双光子共振条件：

$$\omega_p - \omega_c = \omega_2 - \omega_1$$

AC stark 劈裂位置：
缀饰态结构.



理论

In the dipole, rotating-wave and Weisskopf-Wigner approximations, the state vectors $A_1(t)$, $A_2(t)$, $B_1(t)$, and $B_2(t)$ obey the Schrodinger equations [20]:

$$\frac{d}{dt}A_1(t) = -(i\Delta_{11} + \frac{\gamma_{11} + \gamma_{12}}{2})A_1(t) - \frac{\kappa_1 + \kappa_2}{2}A_2(t) - i\Omega_{11}B_1(t) - i\Omega_{12}B_2(t), \quad (2a)$$

$$\frac{d}{dt}A_2(t) = -(i\Delta_{21} + \frac{\gamma_{21} + \gamma_{22}}{2})A_2(t) - \frac{\kappa_1^* + \kappa_2^*}{2}A_1(t) - i\Omega_{21}B_1(t) - i\Omega_{22}B_2(t), \quad (2b)$$

$$\frac{d}{dt}B_1(t) = -i\Omega_{11}^*A_1(t) - i\Omega_{21}^*A_2(t), \quad (2c)$$

$$\frac{d}{dt}B_2(t) = -i(\Delta_{11} - \Delta_{12})B_2(t) - i\Omega_{12}^*A_1(t) - i\Omega_{22}^*A_2(t). \quad (2d)$$

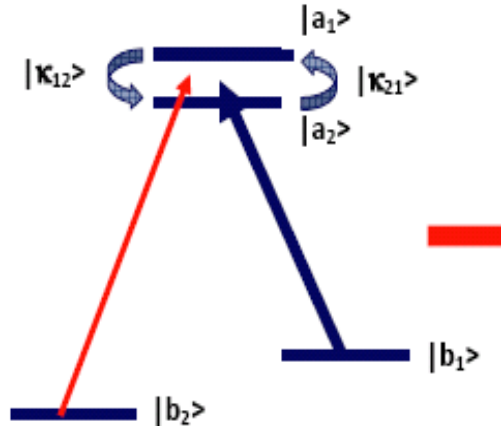
新囚禁条件: $C=C1 \cup C2$

C1: 双光子共振条件

C2: 粒子囚禁条件

与透明点类似

$$|\Omega_{11}\Omega_{22} - \Omega_{12}\Omega_{21}|^2 - (\Delta_{11} - \Delta_{12})(\Delta_{11}|\Omega_{21}|^2 + \Delta_{21}|\Omega_{11}|^2) \\ + i(\Delta_{11} - \Delta_{12})\left(\frac{\gamma_{11} + \gamma_{12}}{2}|\Omega_{21}|^2 + \frac{\gamma_{21} + \gamma_{22}}{2}|\Omega_{11}|^2 - \frac{\kappa_1 + \kappa_2}{2}\Omega_{11}^*\Omega_{21} - \frac{\kappa_1^* + \kappa_2^*}{2}\Omega_{11}\Omega_{21}^*\right) = 0.$$



$$\Delta_{11} = \omega_{a_1 b_1} - \nu_c \text{ and } \Delta_{21} = \omega_{a_2 b_1} - \nu_c.$$

$$\Delta_{12} = \omega_{a_1 b_2} - \nu_p, \Delta_{22} = \omega_{a_2 b_2} - \nu_p,$$

相互作用哈密顿量：

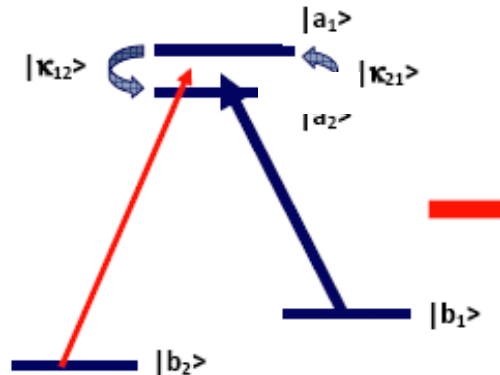
$$H_{int} = \hbar\Delta_{11}|a_1\rangle\langle a_1| + \hbar\Delta_{21}|a_2\rangle\langle a_2| + \hbar(\Delta_{11} - \Delta_{12})|b_2\rangle\langle b_2| \\ + (\hbar\Omega_{11}|a_1\rangle\langle b_1| + \hbar\Omega_{21}|a_2\rangle\langle b_1| + \hbar\Omega_{12}|a_1\rangle\langle b_2| + \hbar\Omega_{22}|a_2\rangle\langle b_2| + H.c.).$$

弱探测光，得到：

$$\Gamma_{D_i} = \frac{1}{\omega_{12}(\lambda_i - \lambda_j)(\lambda_i - \lambda_k)} [(\gamma_{11} + \gamma_{12})(\lambda_i - \Delta_{21})(\lambda_j - \Delta_{11})(\lambda_k - \Delta_{11}) \\ - (\gamma_{21} + \gamma_{22})(\lambda_i - \Delta_{11})(\lambda_j - \Delta_{21})(\lambda_k - \Delta_{21}) \\ + (\kappa_1 + \kappa_2)(\lambda_i - \Delta_{11})(\lambda_j - \Delta_{11})(\lambda_k - \Delta_{11})\frac{\Omega_{21}}{\Omega_{11}} \\ - (\kappa_1^* + \kappa_2^*)(\lambda_i - \Delta_{21})(\lambda_j - \Delta_{21})(\lambda_k - \Delta_{21})\frac{\Omega_{11}}{\Omega_{21}}],$$

三峰的线宽取决于Rabi 频率, 失谐 , 各向异性弛豫速率, 交叉驰豫, 和上能级的间距.

三峰EIT光谱的线宽控制



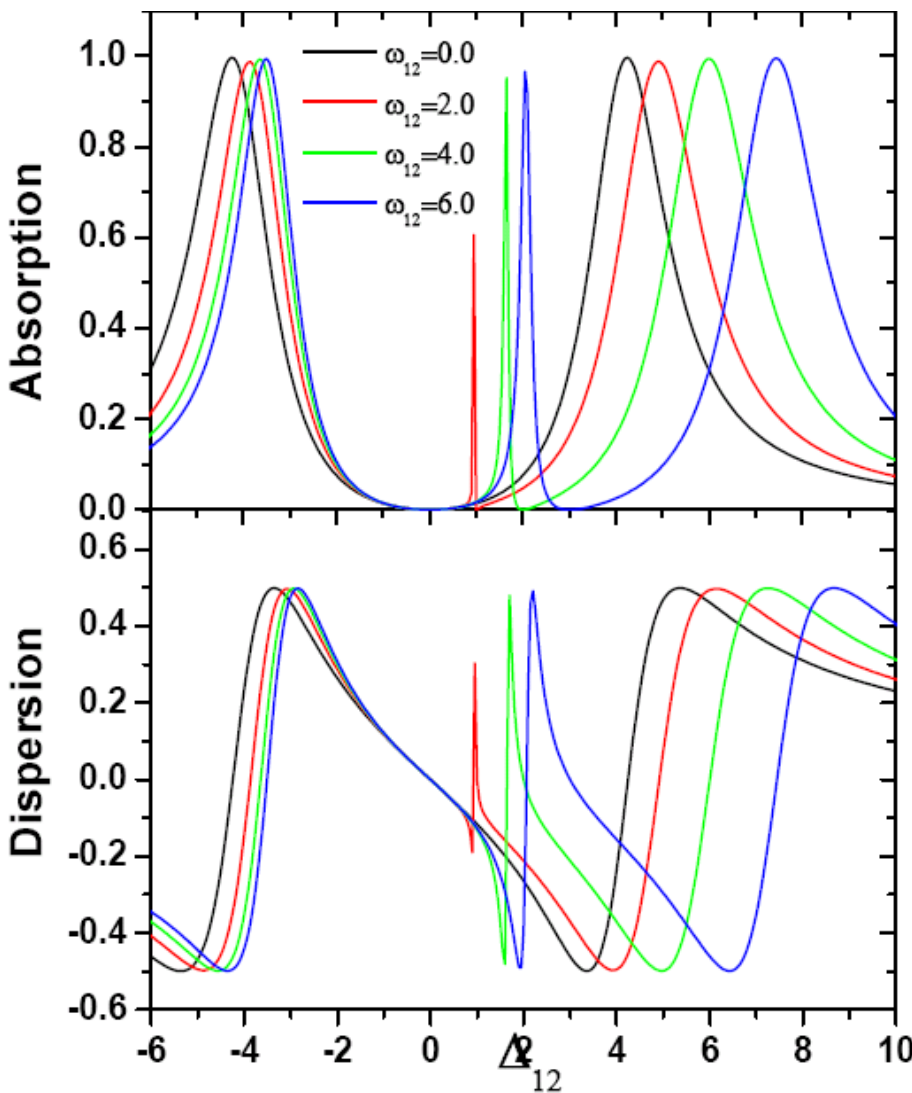
两平行偶极子

1. 出现新的透明点.

Y. J. Zhen et al. PHYSICAL
REVIEW A 83, 013810 (2011).

2. 峰位置与哈密顿量本征值一
致.

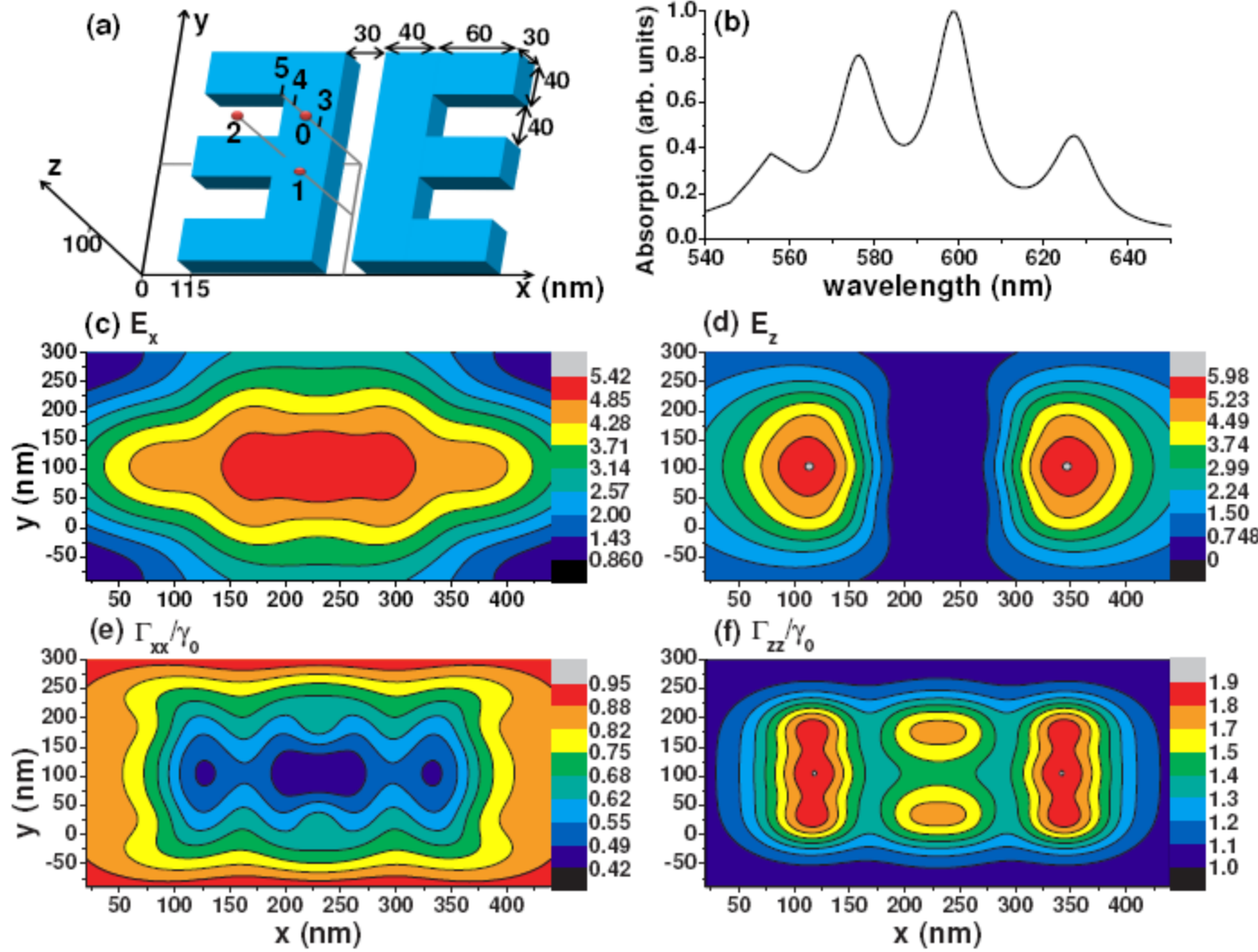
3. 线宽受上能级间距影响明显
linewidths are very sensitive to
the spacing between two upper
levels.

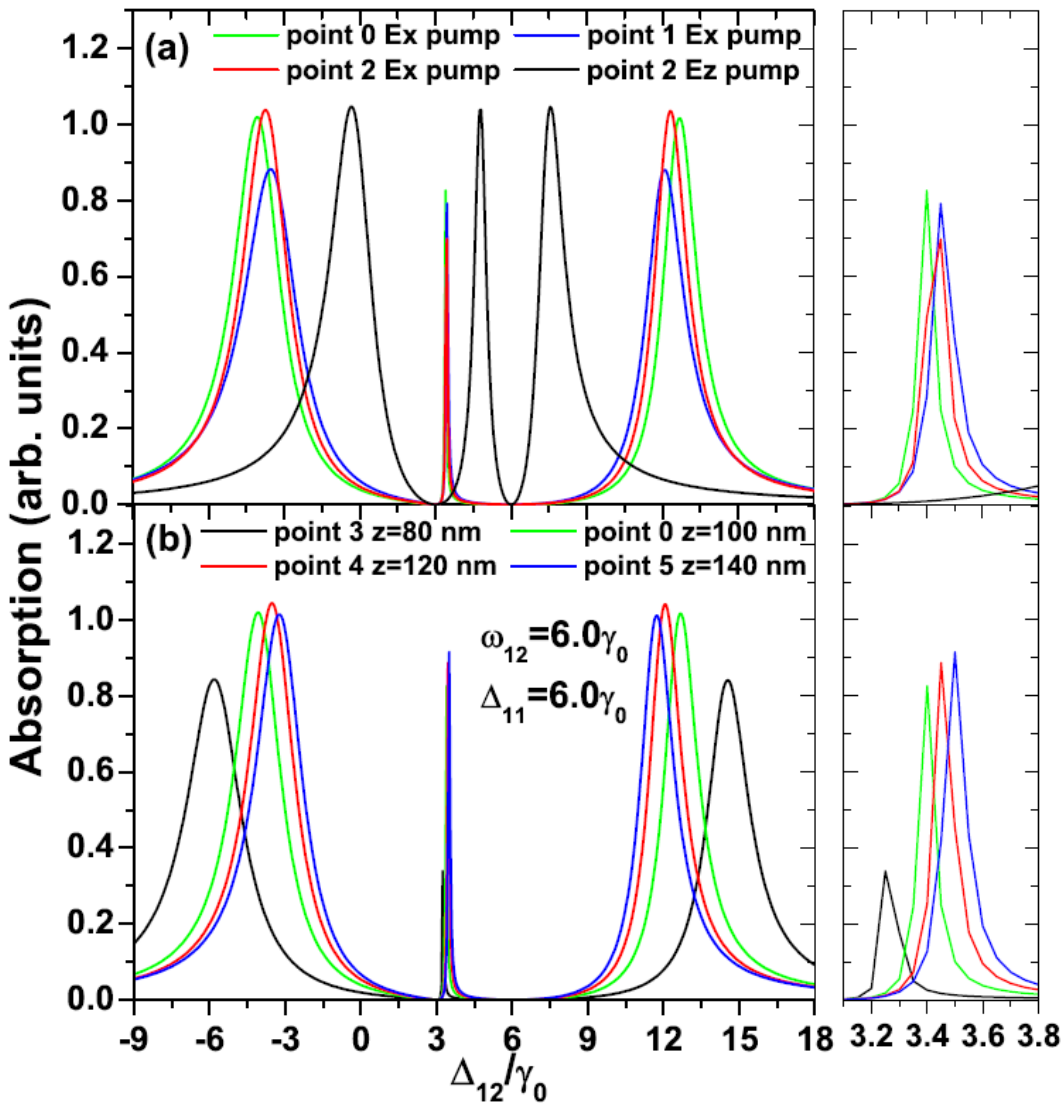


$$\Omega_c = 3.0, \Delta_{11} = 0.0$$

$$\theta_{11} = 0.0\pi, \theta_{12} = 0.0\pi, \theta_{21} = 0.0\pi, \theta_{22} = 0.0\pi$$

共振表面能力激元微腔的偏振EIT





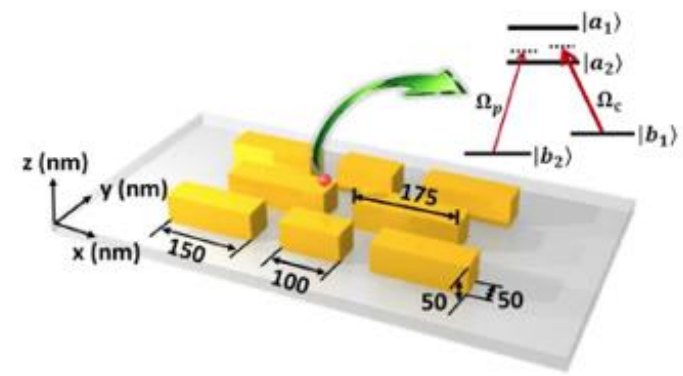
1. 偏振 EIT
2. 线宽控制

提出纳米尺度复合结构克尔非线性的调控

纳米尺度非线性光学平台是实现芯片上量子信息处理的重要部分之一

存在的问题：

1. 传统的非线性体材料受限于其自身体积因素，阻碍了技术的发展
2. 利用自发诱导相干效应对克尔非线性的调控，受限于非垂直偶极矩情形，实验实现困难



Sci.Rep. (2015)

我们的解决方案

提出表面等离激元和量子发射体复合结构，达到在纳米尺度实现对于克尔非线性效应的有效调控目的

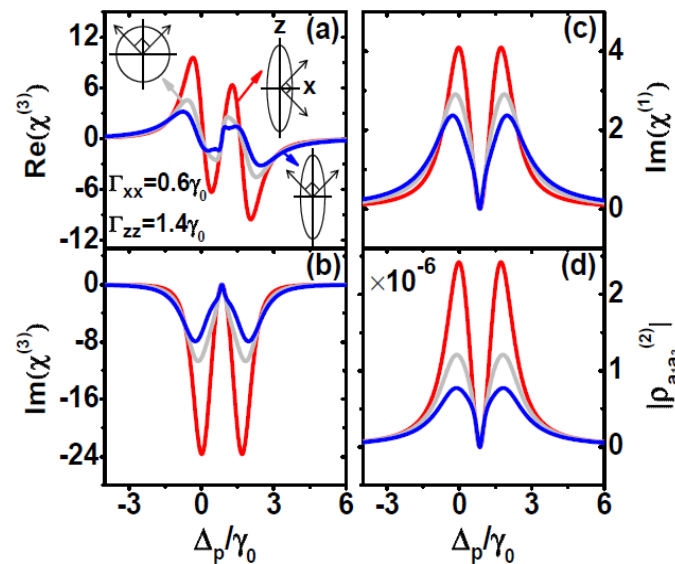
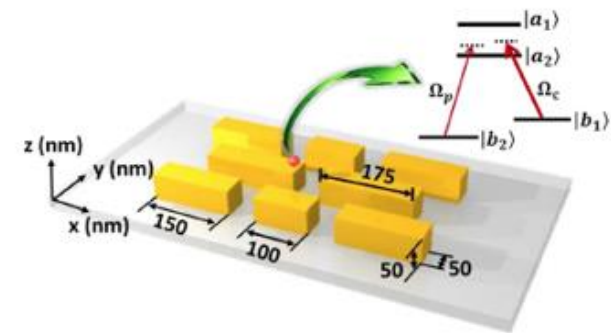
调控机理：

利用量子发射体与光场的相干相互作用
以及表面等离激元结构提供亚波长尺度
的各向异性珀塞尔系数，使得垂直偶极矩
情形，增强自发诱导相干效应

达到：

在纳米尺度对于克尔非线性效应的
依赖于原子空间位置的有效调控

有望作为芯片上非线性光学器件

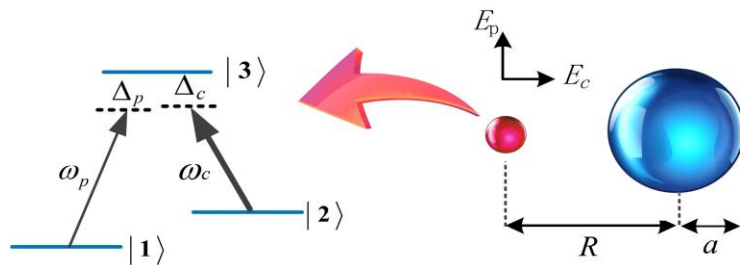
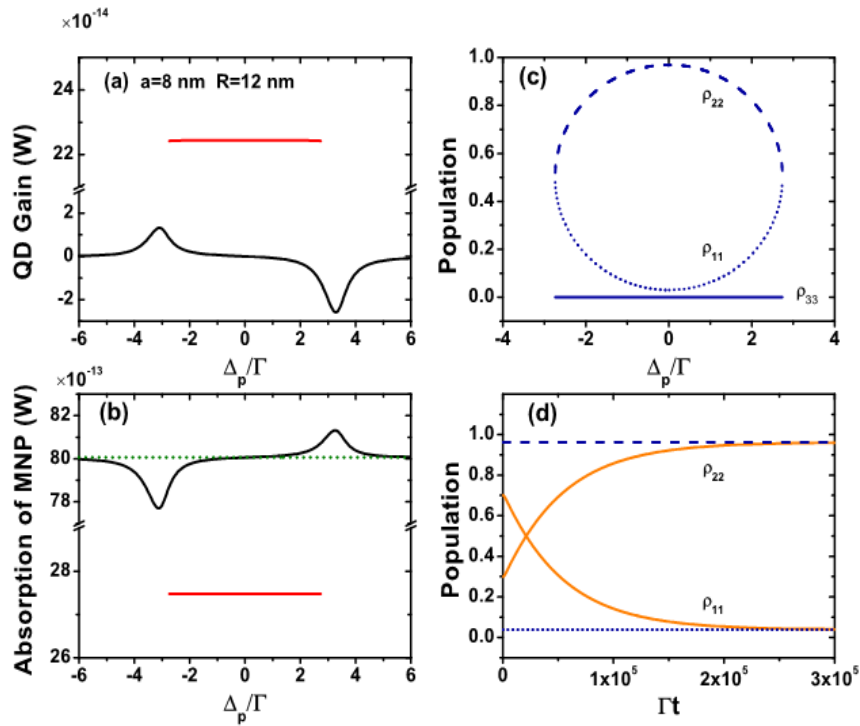


- 弱耦合范畴
 - 高效方向性单光子发射
 - 各向异性珀赛尔系数组调量子相干性质
-
- 中等强度耦合范畴
 - 借助于表面等离激元的无粒子数反转增益
-
- 强耦合范畴
 - 條逝波下的耦合因子增强

在中等强度耦合区域，预测杂化体系中新奇量子效应，如
金属颗粒辅助的无布居数反转增益效应
激子通道借助表面等离激元裁剪的Fano线型

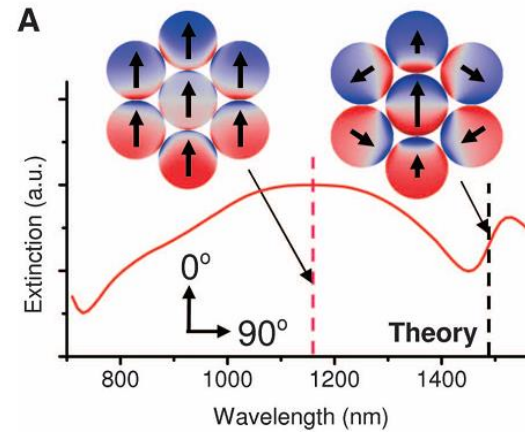
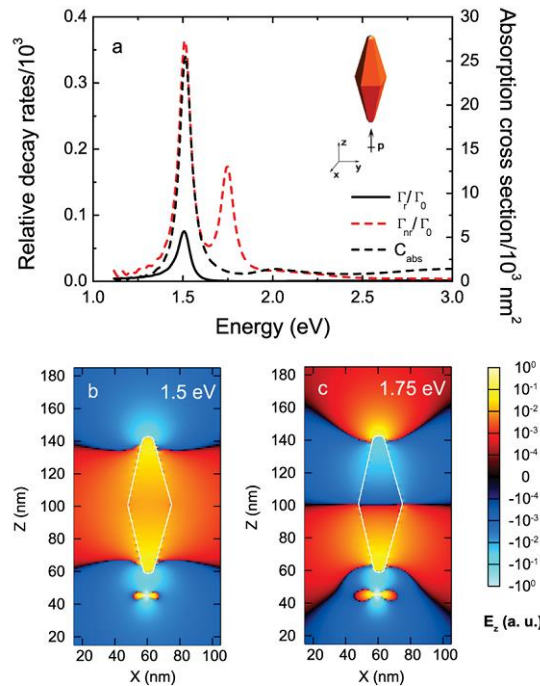
PRB(2014), Appl.Phys.Lett.(2014), PRA (2015)

金属颗粒辅助的无布居数反转增益效应



什么是暗表面等离激元？

暗表面等离激元：由于偶极矩消失引起的非辐射局域表面等离激元模式

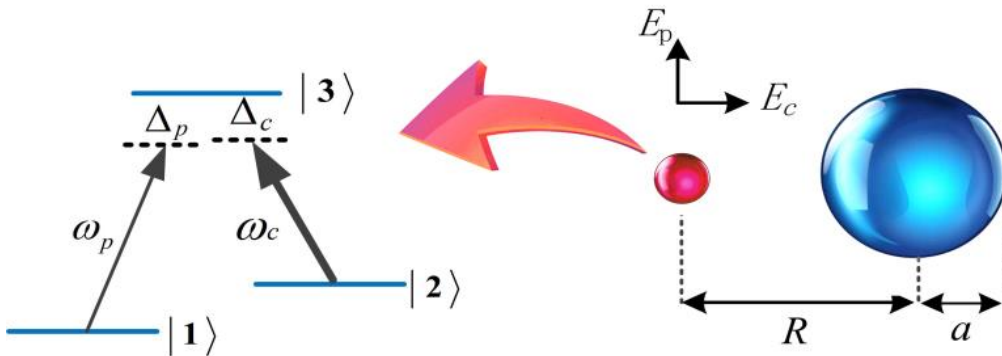


由于近场交叠，
亮模式诱导暗模式

在我们实例中， 暗模式间接地被附近的量子点激发

基本想法：暗表面等离激元如何在QD-MNP相互作用中起作用的？

模型建立



QD作用的三条路径

$$I \rightarrow \mu_{23}^{QD}$$

I : Incident light

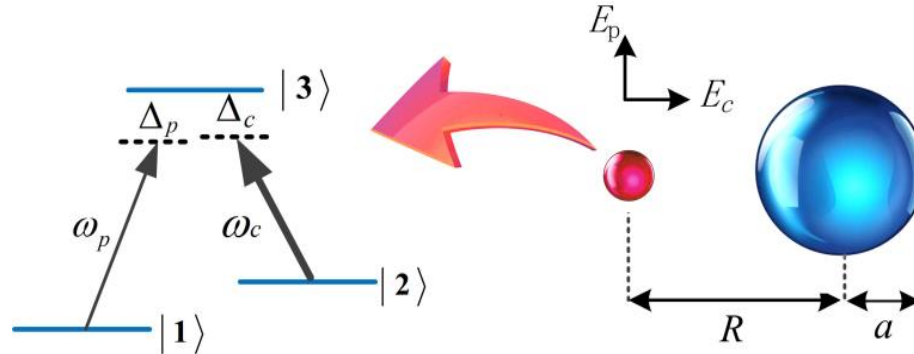
$$I \rightarrow B^{MNP} \rightarrow \mu_{23}^{QD}$$

B^{MNP} : Bright Plasmon of MNP

$$\mu_{23}^{QD} \rightarrow B^{MNP} + D^{MNP} \rightarrow \mu_{23}^{QD}$$

D^{MNP} : Dark Plasmons of MNP

哈密顿量



$$H = \sum_{i=1}^3 \hbar \omega_i \sigma_{ii} - \mu_{23} (\sigma_{23} + \sigma_{32}) E_{23} - \mu_{13} (\sigma_{13} + \sigma_{31}) E_{13}$$

Transition $|2\rangle \leftrightarrow |3\rangle$ is on-resonance with the surface plasmon of MNP

$$E_{23}^+ = (E_1^+ + E_2^+ + E_3^+) e^{-i\omega_c t}$$

$$E_1^+ = \frac{E_c}{2} \quad E_2^+ = \frac{a^3 E_c}{R^3} \alpha_1(\omega_c) \quad E_3^+ = \sum_{n=1}^{\infty} \frac{(n+1)^2 a^{2n+1} \mu_{23} \rho_{32}}{4\pi \epsilon_0 \epsilon_b R^{2n+4}} \alpha_n(\omega_c)$$

亮模式和暗模式的
反馈

Transition $|1\rangle \leftrightarrow |3\rangle$ is off-resonance with the surface plasmon of MNP

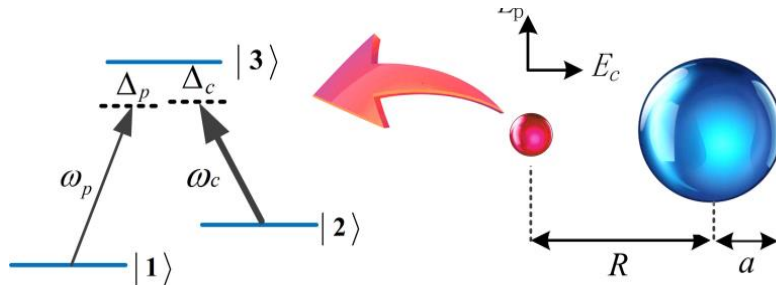
$$E_{13}^+ = \frac{E_p}{2} e^{-i\omega_p t}$$

非线性 Master equation

$$H = \hbar(\Delta_p - \Delta_c)\sigma_{22} + \hbar\Delta_p\sigma_{33} - \hbar[(\Omega'_c + G_c\rho_{32})\sigma_{32} + H.c.] - \hbar(\Omega_p\sigma_{31} + H.c.),$$

$$\Omega'_c = \Omega_c + \frac{\mu_{23}E_2^+}{\hbar} \text{ and } G_c = \frac{\mu_{23}E_3^+}{\hbar}$$

$$\Omega_c = \frac{\mu_{23}E_1^+}{\hbar}$$



$$\dot{\rho} = \frac{i}{\hbar} [\rho, H] + L(\rho)$$

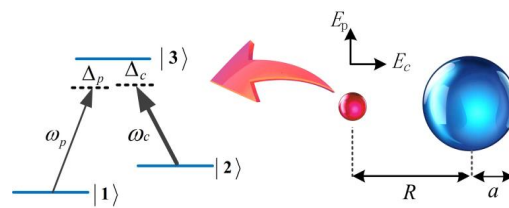
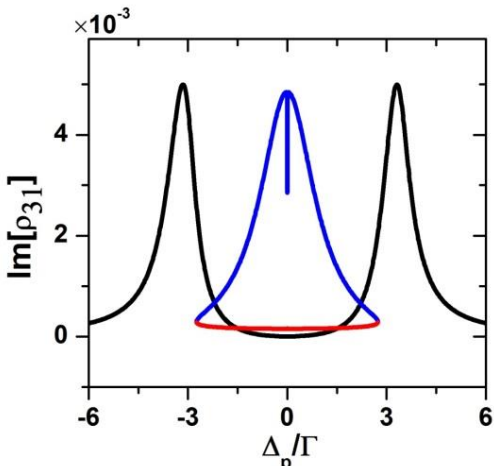
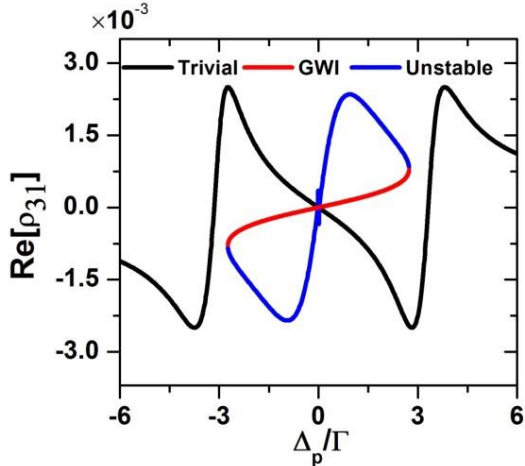
反馈产生非线性效应

$$\dot{\rho}_{31} = -i\Delta_p\rho_{31} + i(\Omega_c + G_c\rho_{32})\rho_{21} - i\Omega_p(\rho_{33} - \rho_{11}) - \frac{1}{2}\gamma_{31}\rho_{31}$$

$$\dot{\rho}_{32} = -i\Delta_c\rho_{32} + i\Omega_p\rho_{12} - i(\Omega_c + G_c\rho_{32})(\rho_{33} - \rho_{22}) - \frac{1}{2}\gamma_{32}\rho_{32}$$

$$\dot{\rho}_{21} = -i(\Delta_p - \Delta_c)\rho_{21} - i\Omega_p\rho_{23} + i(\Omega_c^* + G_c^*\rho_{23})\rho_{31} - \frac{1}{2}\gamma_{21}\rho_{21}$$

多解



3个稳态解

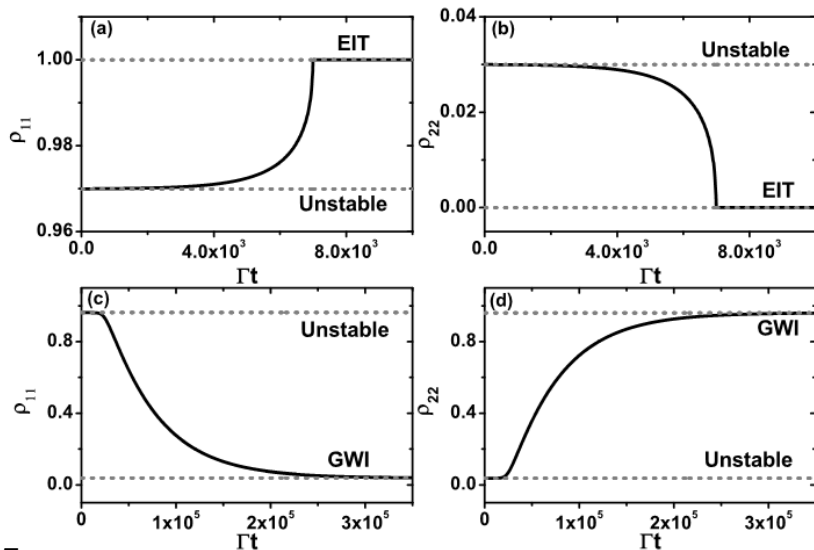
1st EIT 解

2nd 非稳

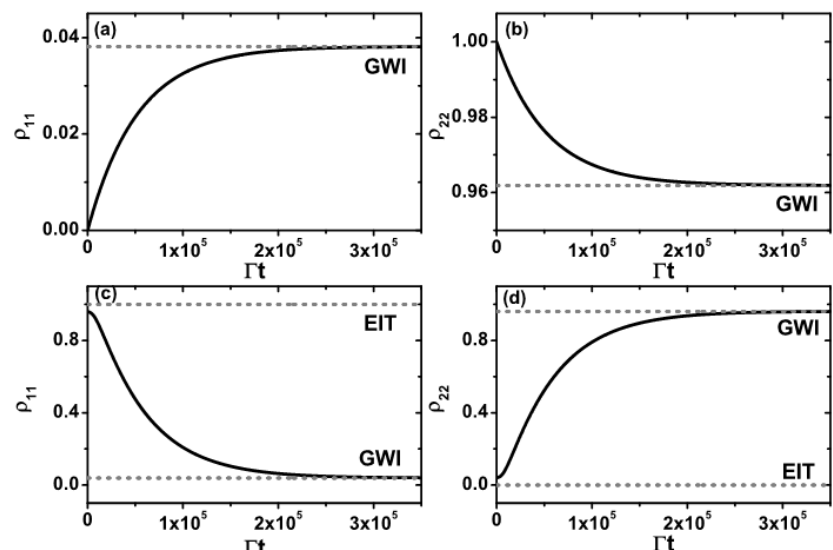
3rd GWI 解

$a = 8 \text{ nm}$, $R = 12 \text{ nm}$, $\Omega_p = 0.005$,
 $\Omega_c = 0.5$, $\omega_{32} = 3.47 \text{ eV}$ and $\Delta_c = 0$.

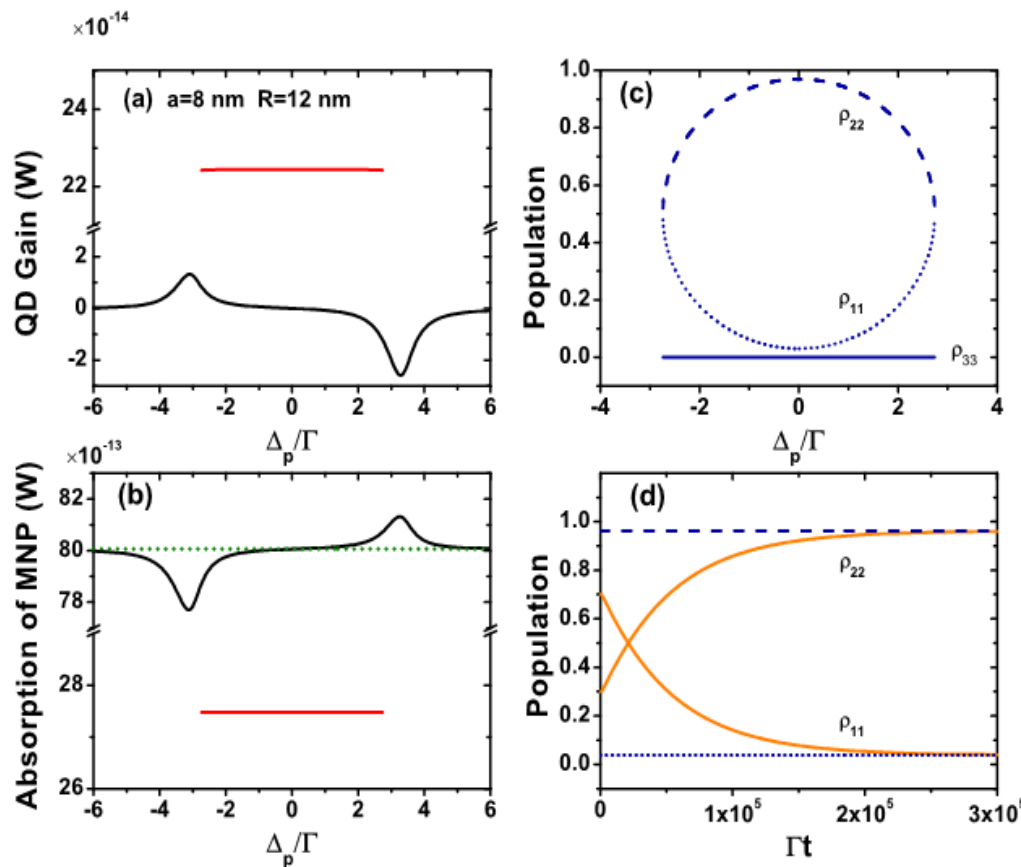
2nd 解 非稳定



3rd 解 较强的作用

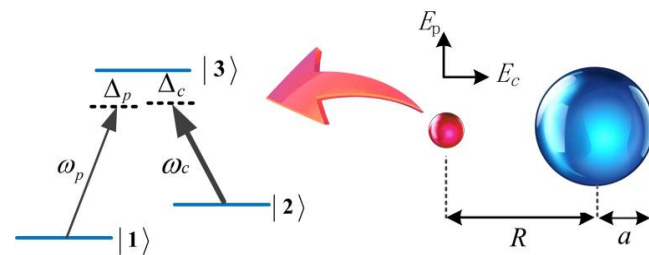


无反转增益(GWI)



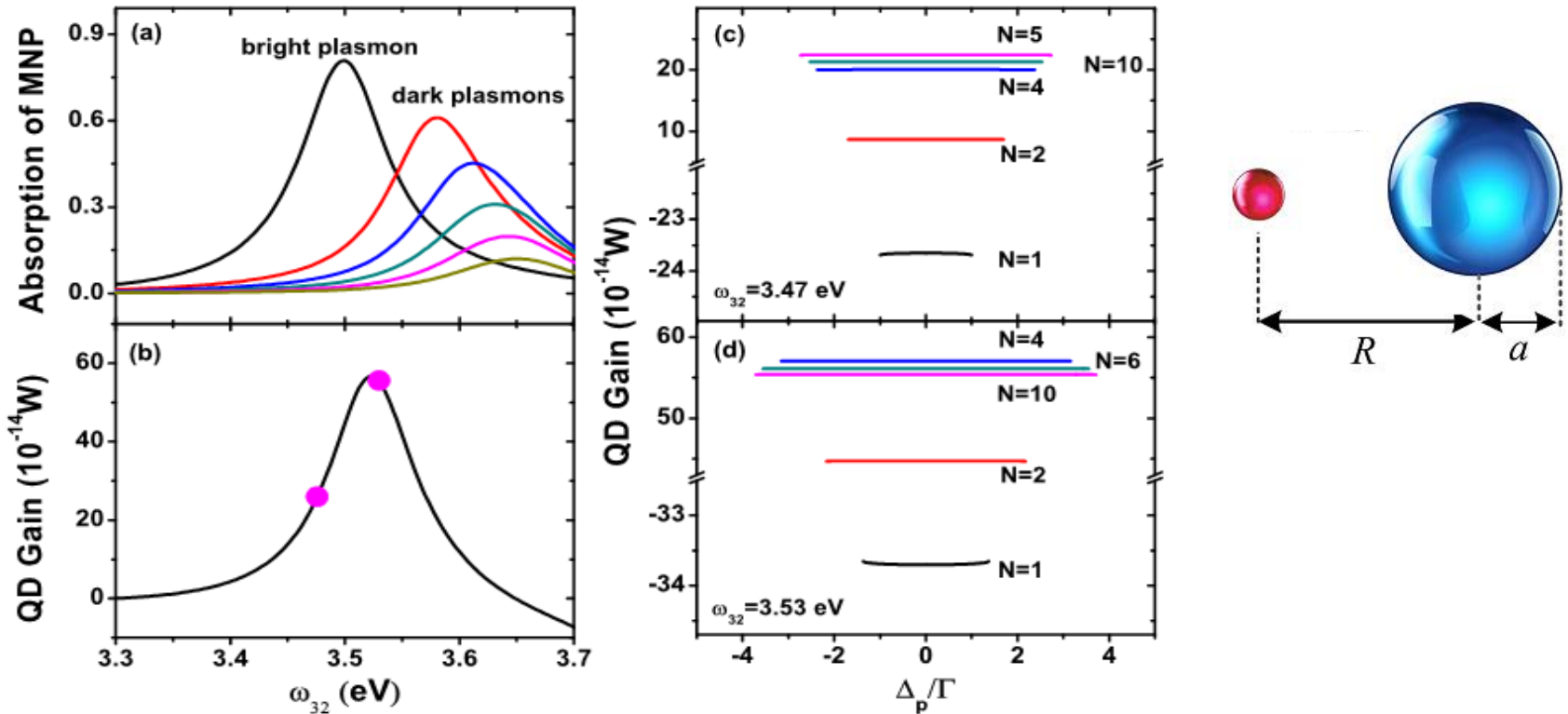
$\Omega_p = 0.005\Gamma$, $\Omega_c = 0.5\Gamma$, $\Delta_c = 0$ and $\Delta_p = -0.5$ (only for (d))

the imaginary part of $-2\hbar\omega_c\Omega_c\rho_{32}$



1. 增益存在于QD的 $|2\rangle \leftrightarrow |3\rangle$ 通道.
2. QD的增益产生于MNP到QD的能量转移过程.
3. 在增益效应中没有粒子数反转.
4. GWI 与初态相关.

暗表面等离激元如何作用？



- 增益产生于MNP暗模式的反馈
- 增益在MNP表面等离激元亮模式和暗模式重叠最大的时候达到最大值。

粒子数反转增益

新的机制: MNP暗表面等离激元的反馈

受初态影响

可调节并且实验可行

可能应用

超紧凑量子点激光器

太阳能电池

量子态制备和粒子数转移

提出局域表面等离激元结构调控量子比特纠缠

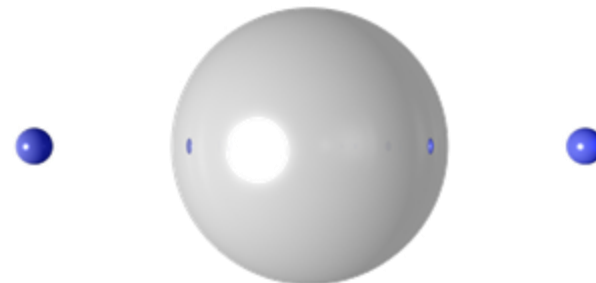
量子纠缠是量子计算、隐形传态、量子通信的基础，实现芯片上量子信息是未来发展的重要方向

目的：

利用表面等离激元局域性质增强量子比特纠缠；
研究失谐对于稳态纠缠的影响

我们的方案：

量子点-金属球-量子点结构；
利用量子点与金属球之间的反馈作用



结果：

金属球结构可以有效增强纠缠(1-3

个数量级)；

量子点-金属球-量子点结构中失谐
存在有效增强纠缠(达到5.3倍)。

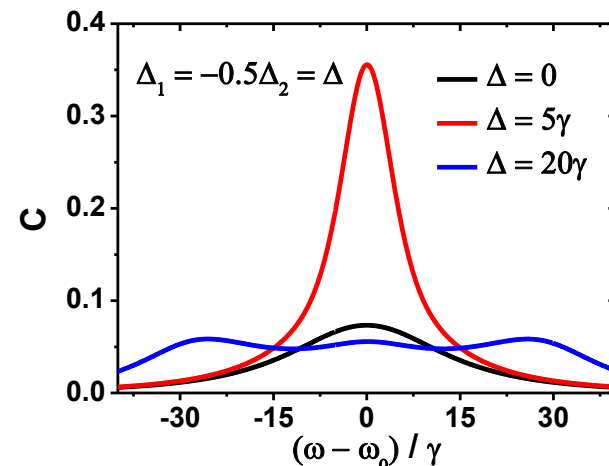
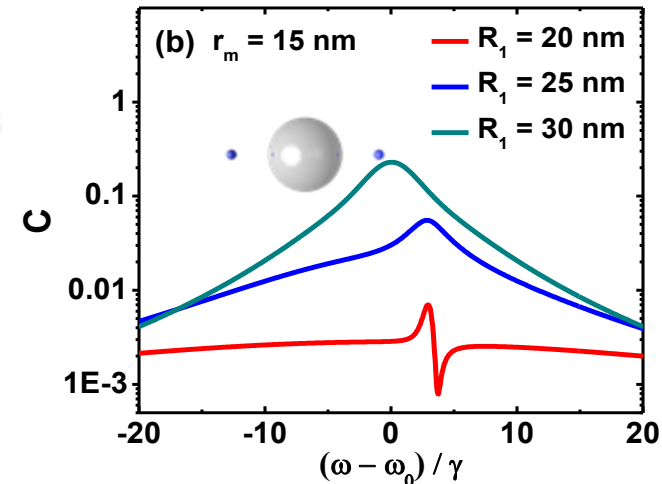
意义：

有利于实现高效稳态纠缠；

体积小，有利于实现芯片上量子信
息功能。

Concurrence

$$C(\rho) = \max\{\lambda\sqrt{1-\lambda^2} - \lambda\sqrt{3-\lambda^2}, 0\}$$



倏逝波调控金属球-量子发射体结构纠缠

集成量子
芯片对纠
缠要求

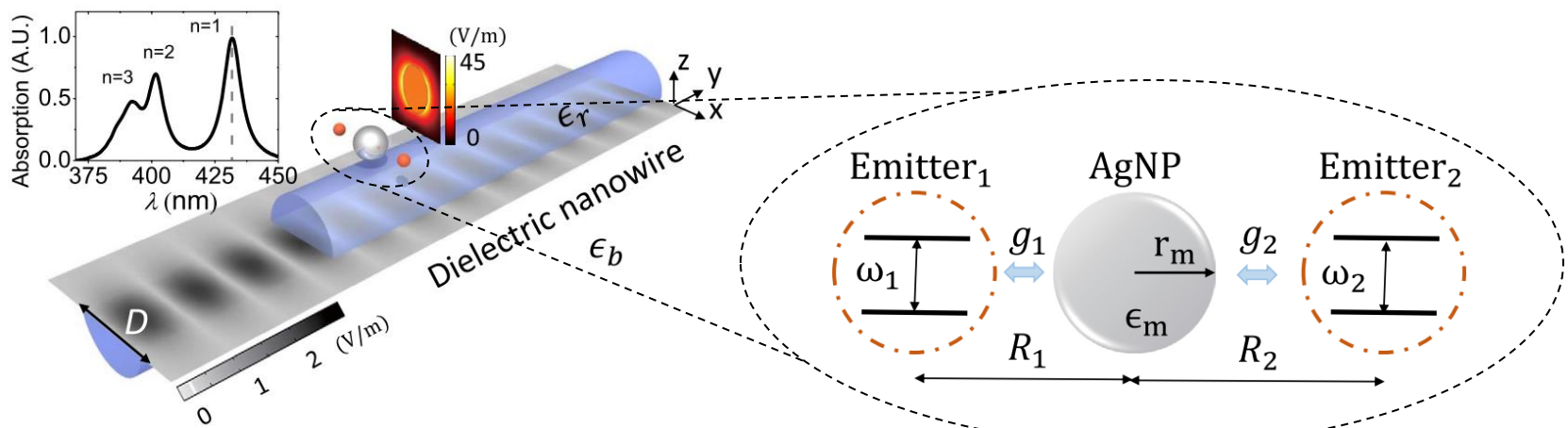
1. 单光子水平更
大的光与物质相
互作用

2. 有效的激发和
传导信息

增强耦合

纳米光
子结构

倏逝场代替
平面波
调控金属球
-量子发射
体结构纠缠

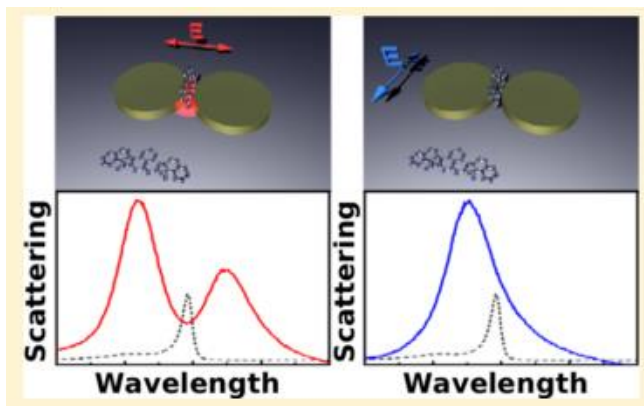


- 弱耦合范畴
 - 高效方向性单光子发射
 - 各向异性珀赛尔系数组调量子相干性质
-
- 中等耦合范畴
 - 倏逝波下的耦合因子增强
-
- 强耦合范畴
 - 倏逝波下的耦合因子增强

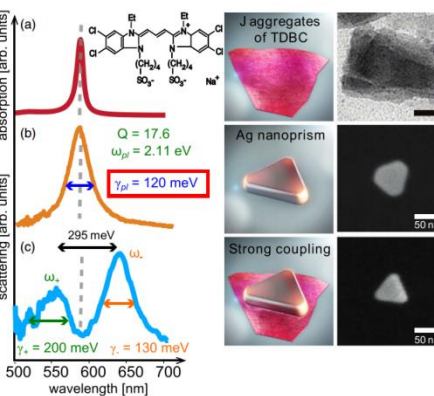
倏逝波增强量子体系 / 表面等离激元相互作用

CQED强耦合在量子信息方面有潜在应用，如可以把原子作为量子存储节点，而光子成为飞行量子比特。

但是为了集成以及可扩展的需要，必须发展模式体积更小的腔



Nano Lett. 2013, 13, 3281



实验上实现的多个分子和表面等离激元结构的强相互作用

$$g = \frac{\vec{\mu} \cdot \vec{E}}{\hbar}$$

PRL 114, 157401 (2015)

由于表面等离激元的内禀损耗以及低的收集和传导效率，真正单个表面等离激元结构和单个原子的强耦合没有实现。

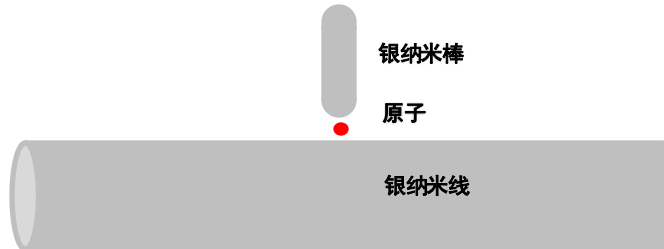
基本想法

各向同性真空



VS

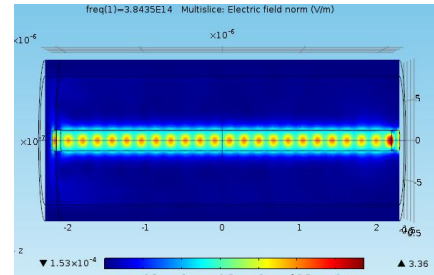
倏逝电磁真空



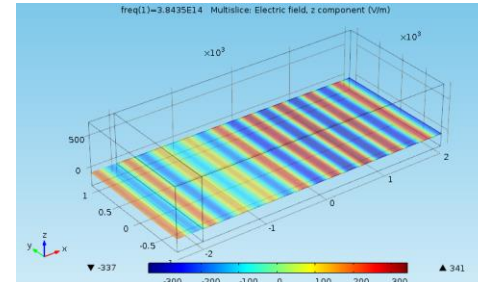
倏逝波被局域在一维（对于纳米光纤和金属纳米线）或二维（金属薄膜或金属板）空间中，所以倏逝波下表面等离激元结构的模式会比在真空中更加局域

- (1) 更加局域的电磁场可以增强耦合因子
- (2) 可以通过倏逝波有效的收集和传导光子

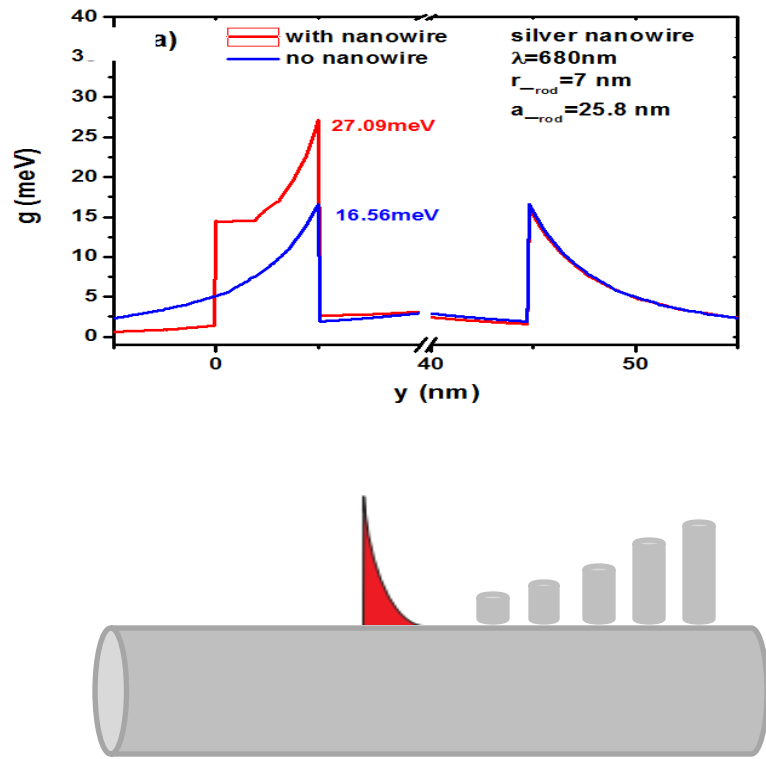
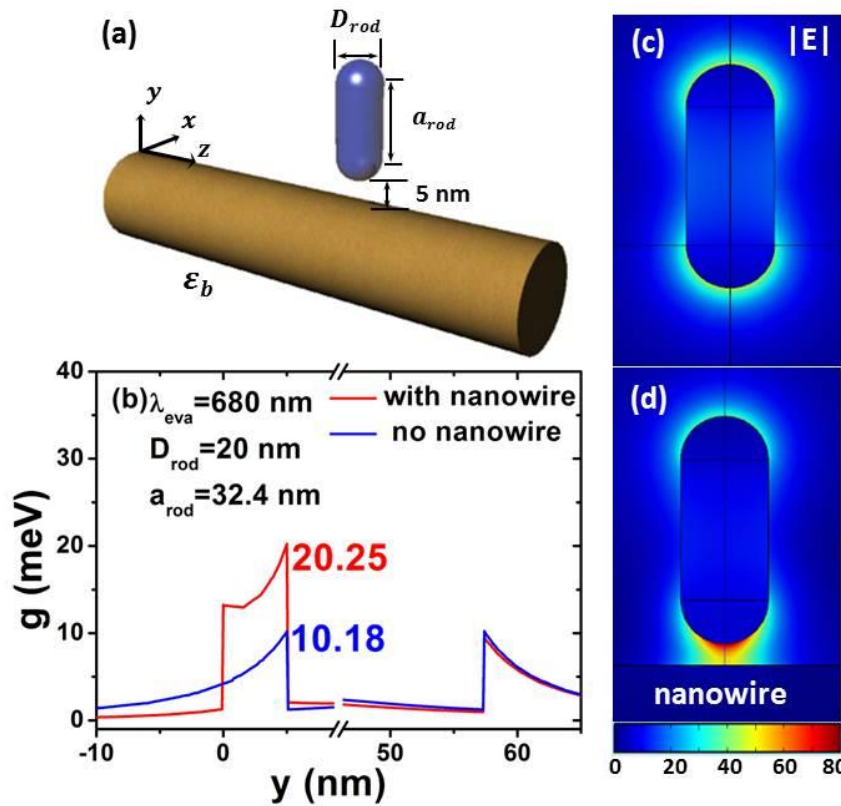
nanofiber



Metallic layer

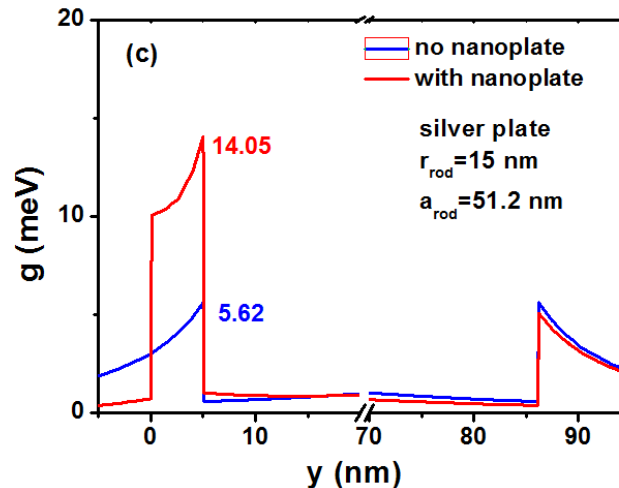
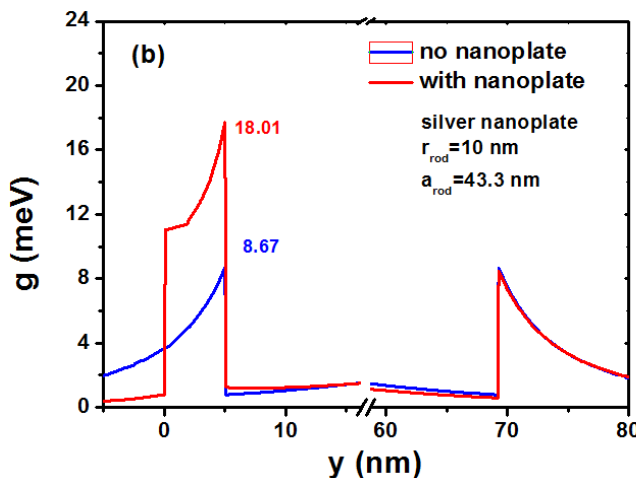
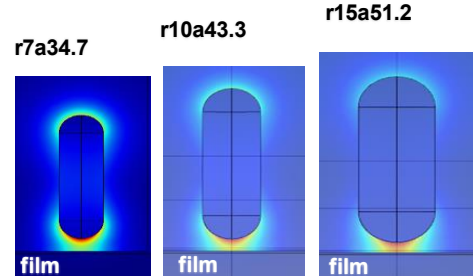
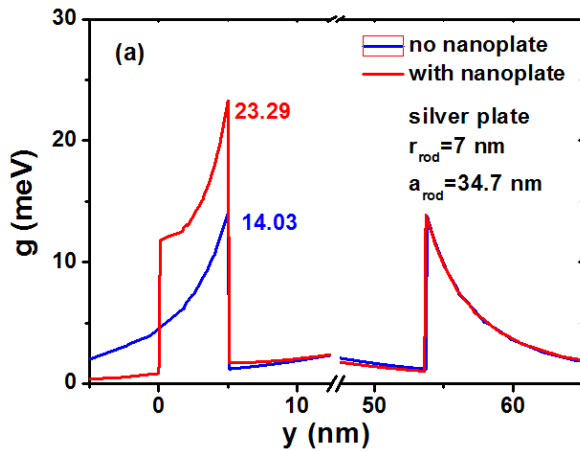


通过银纳米线增强耦合因子



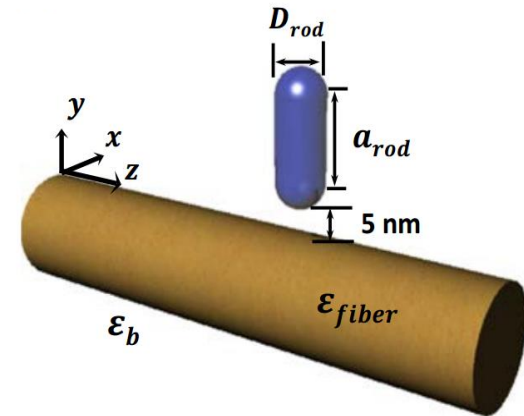
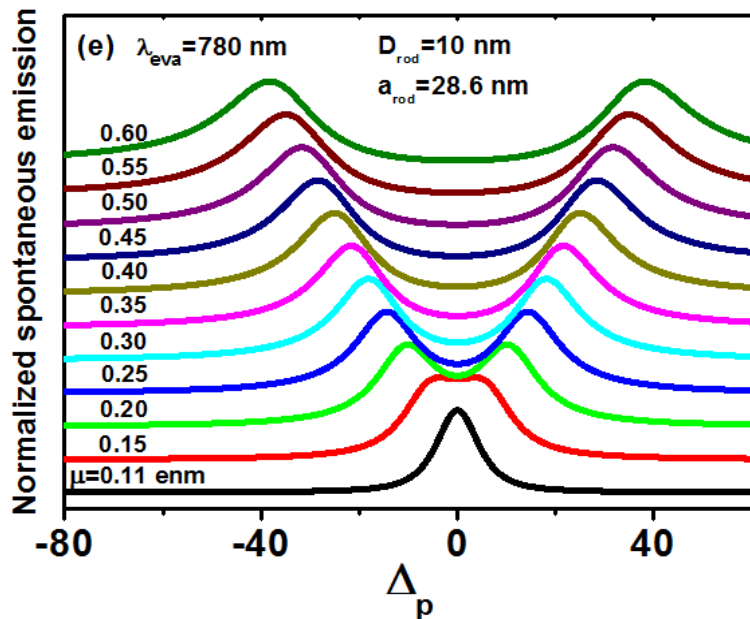
- (1) 耦合因子分别是没有银纳米线时的1.99倍(b)和1.64倍(e)
- (2) 长银纳米棒受倏逝波的影响更大，这是因为长的纳米棒可以感受到更大的电场倏逝

通过银膜增强耦合因子



分别是没有银膜的1.66倍(a)(2.08倍(b), 2.5倍(c))

拉比劈裂，光子的有效传导和收集



变化量子发射体的电偶极矩
所得自发辐射谱，当为原子
偶极矩时，出现拉比劈裂

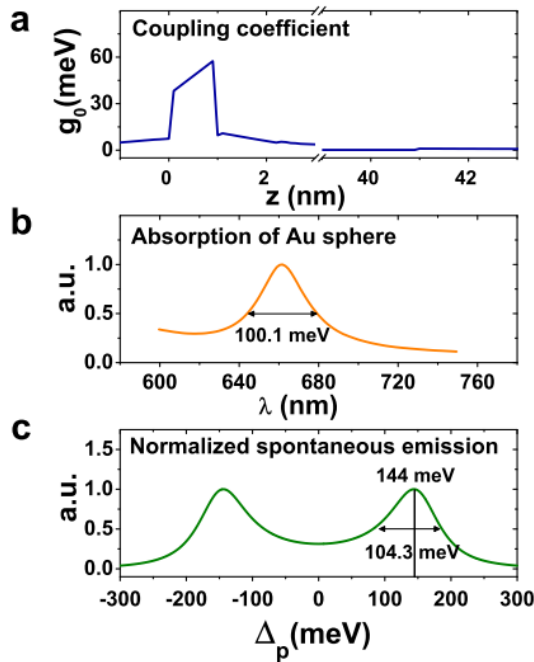
$$\eta = \frac{\Gamma_{ev}}{\Gamma_{total}}$$

传导效率为 30%-70%.

Y. Gu et al. PRL 118,
073604 (2017)

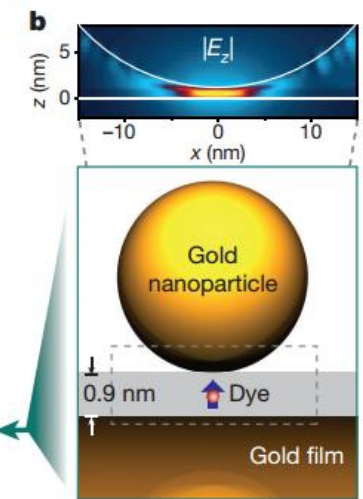
$(\lambda, D_{rod}, a_{rod}) \text{ (nm)}$	channeling efficiency
680, 10, 21.2	30.94 %
680, 14, 27.8	52.06 %
680, 20, 36.5	71.94 %
600, 10, 15.3	20.03 %
780, 10, 28.6	40.06 %

实验支持



耦合系数（对于1个emitter）

$$g_0^{mid} = 47.84 \text{ meV} \text{ vs } g_0 = 45 \text{ mev}$$



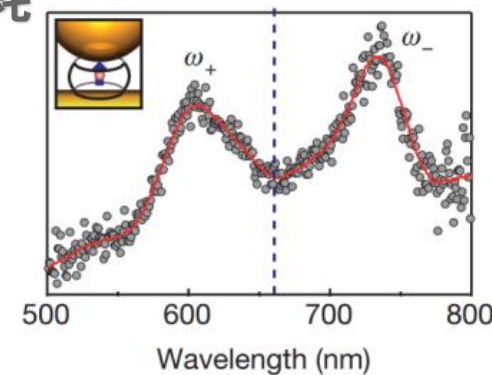
共振波长, 表面等离激元微腔损耗

$$\lambda = 660 \text{ nm} \text{ vs } 660 \pm 10 \text{ nm}$$

$$\kappa = 100.1 \text{ mev} \text{ vs } 122 \text{ mev}$$

拉比频率（对于10个emitter）

$$288 \text{ meV} \text{ vs } 300 \text{ meV}$$



Nature 535, 127
(2016)

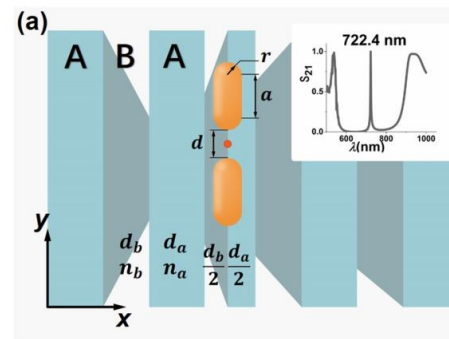
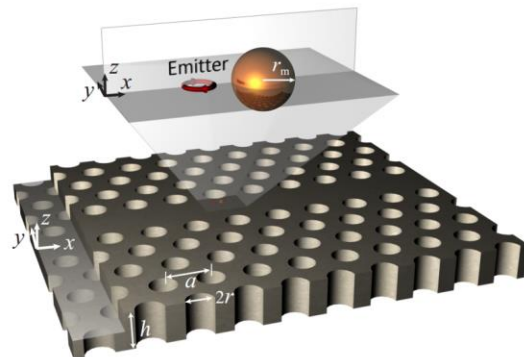
- 1 为我们的理论工作提供了实验支持（结构制备，距离控制等）
- 2 我们更加清晰地阐述了疏逝真空增强耦合系数的机制：对更长金属颗粒的的耦合系数增强越大（而这里金纳米球大小是固定的）
- 3 利用疏逝真空进行收集和传导光子

- 解析求解表面等离激元的方法及应用
- 基于表面等离激元光学的CQED及应用
- 基于复合纳米结构的CQED

基于复合纳米结构的CQED

一、微纳光子结构中光子-激子手性耦合

二、拓扑保护下珀塞尔效应

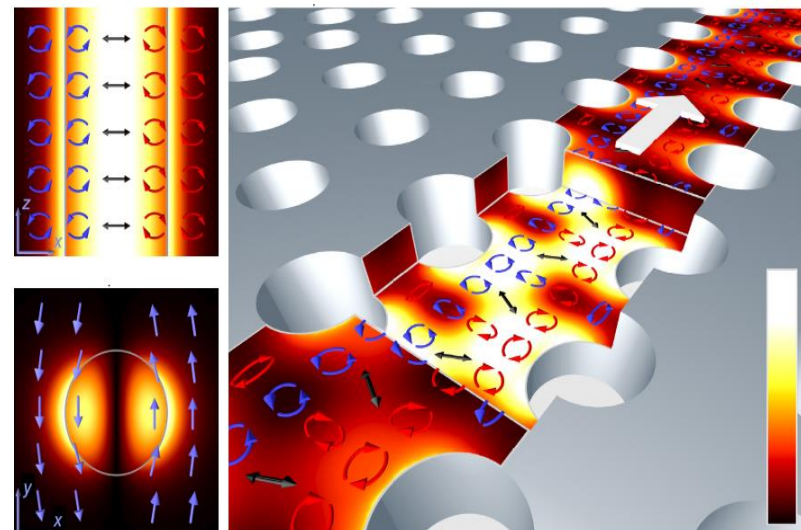
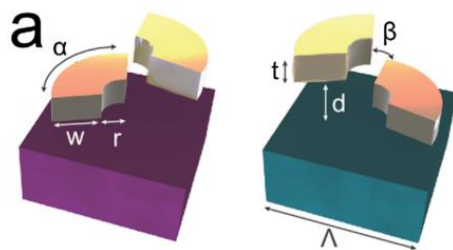
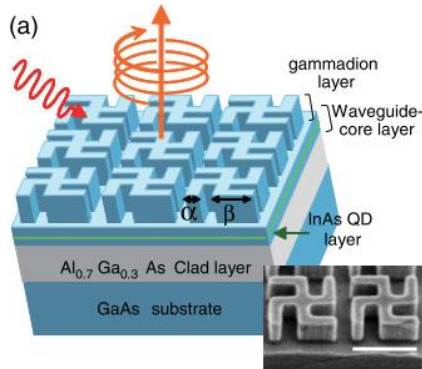


一、微纳光子结构中的光子和激子的手性耦合

Various “Chirality”

Chiral structures

Chiral electric field in PC

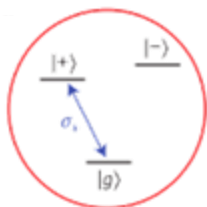


PRL, 106, 057402(2011)
nanoscale, 6 14244 (2014)

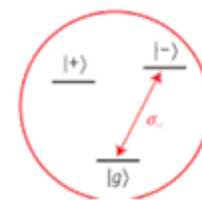
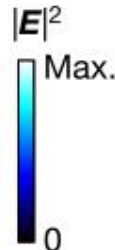
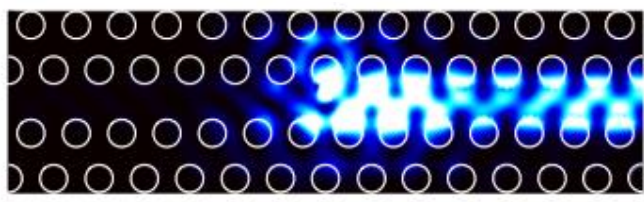
Nature 541, 473(2017).

Chiral photon- emitter coupling

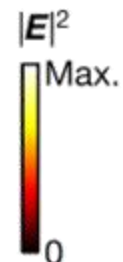
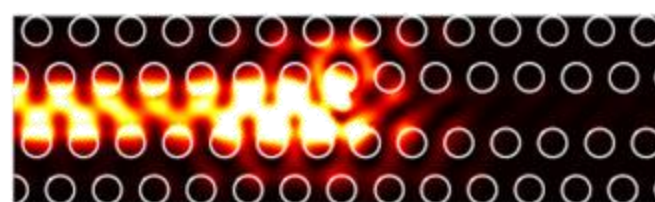
When a circularly polarized emitter placed near these structures?



Left-handed
polarized emitter



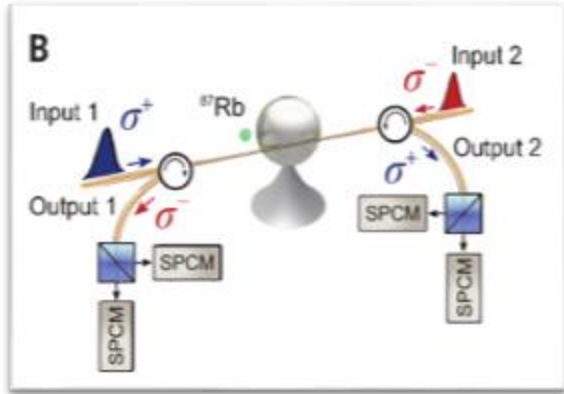
Right-handed
polarized emitter



Lock the local polarization of the light to its propagation direction, so called spin-locked propagation

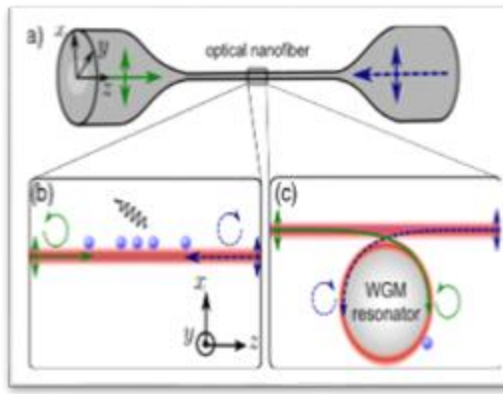
Various nonreciprocal quantum circuits

Switching



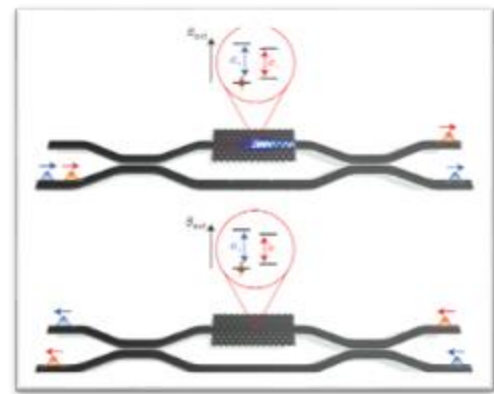
Science 345, 903 (2014)

Isolator



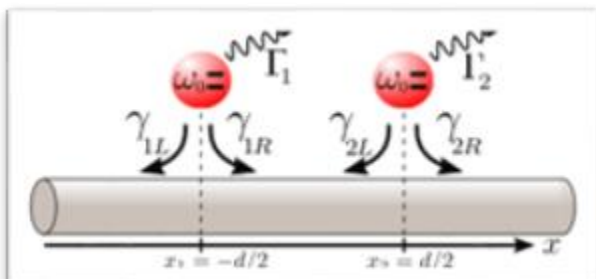
PRX 5, 41036 (2016)

Quantum gate



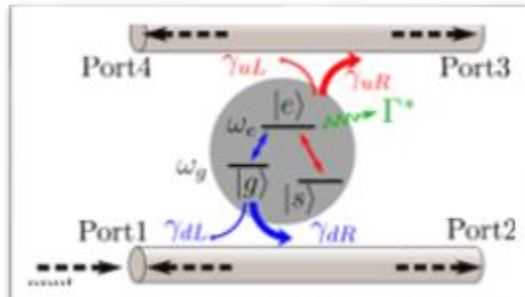
Nat. Nanotechnol. 10, 775(2015)

Entanglement



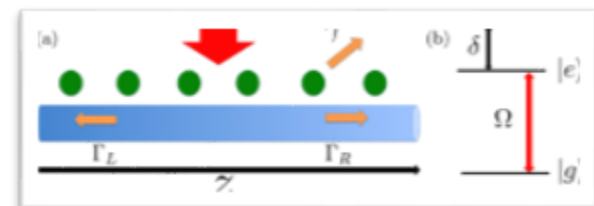
PRB 92, 155304 (2015)

Routing



PRA 94, 063817(2016)

Trapping



PRA 94, 53855 (2017)⁶³

Motivation

at the nanoscale ?

Coupling
strength of
photon-emitter

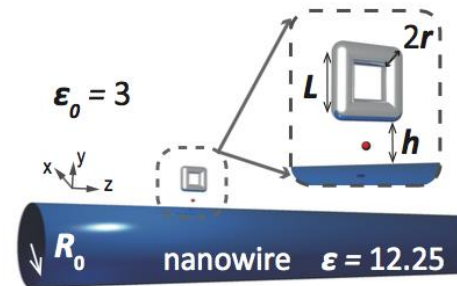
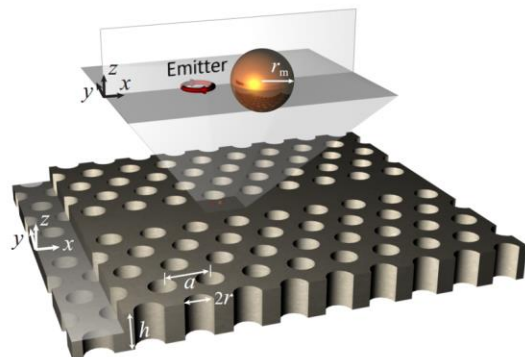


Spin-locked
photon
propagation

Nano-CQED

Chiral coupling

Solution: coupled nanophotonic structures



Mode coupling between PC and AgNP

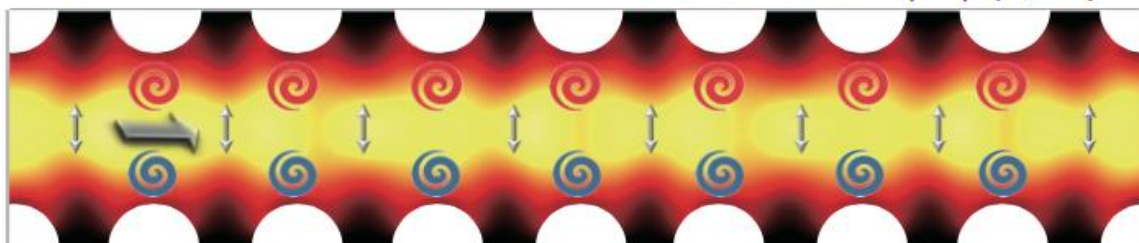
Strong local field with high electric helicity

Helicity of z direction:

$$\frac{2\text{Im}[E_x E_y^*]}{|E_x|^2 + |E_y|^2}$$

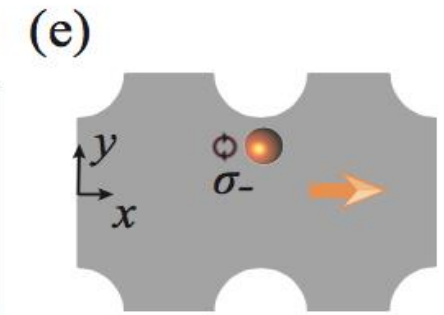
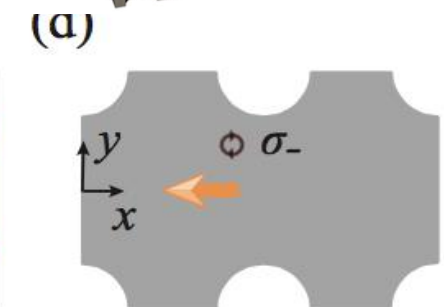
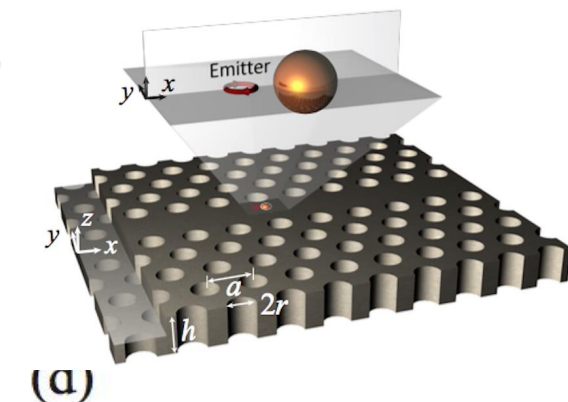
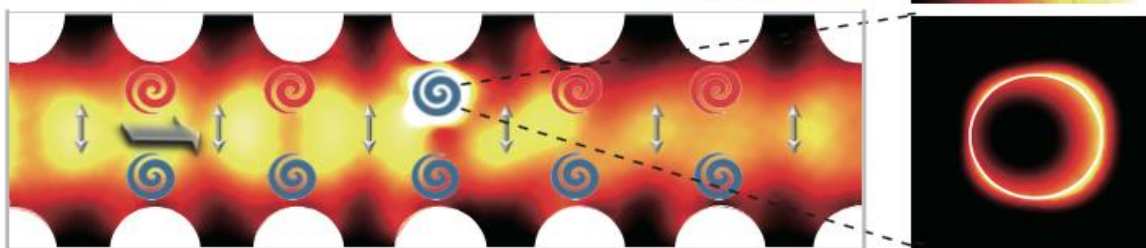
(b) only PC

50 220 $|E|$ (V/m)



(c) PC + AgNP

50 220 1000 3500



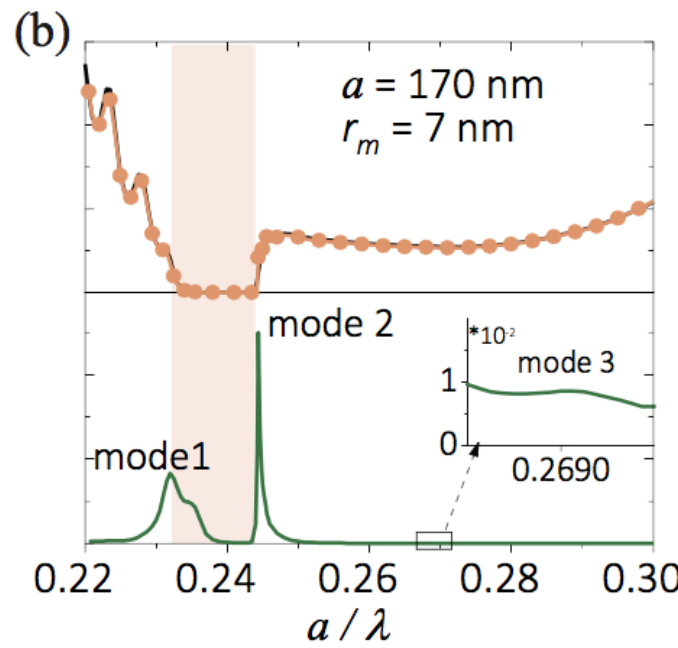
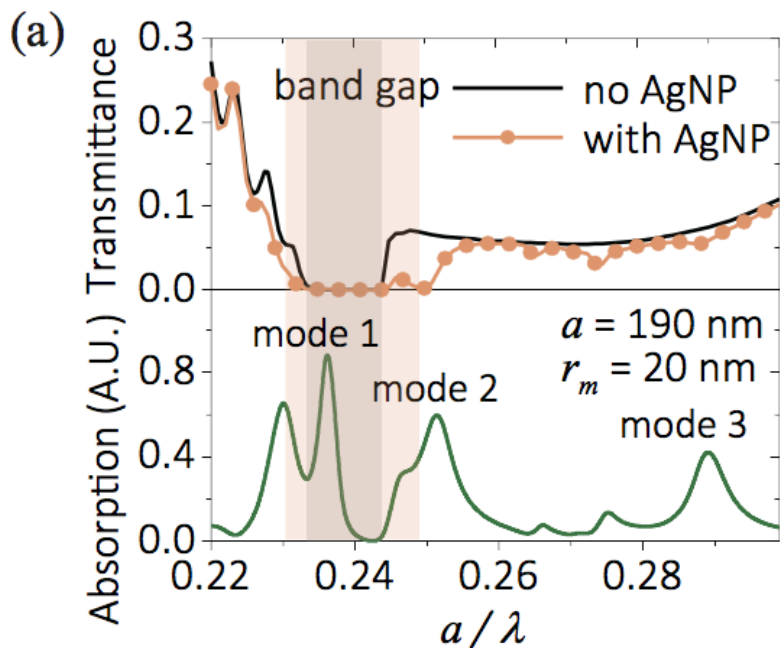
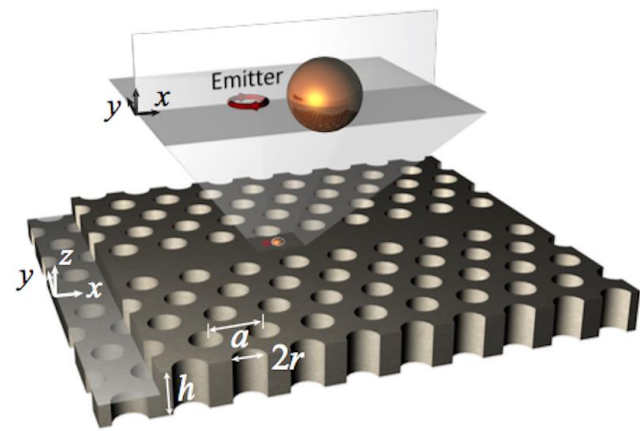
Result of mode coupling

For PC: The shift of Bandgap

For AgNP: mode 1

mode 3 for Purcell enhancement

mode 2 for Rabi splitting bandedge mode



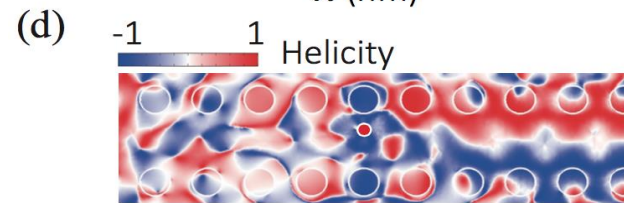
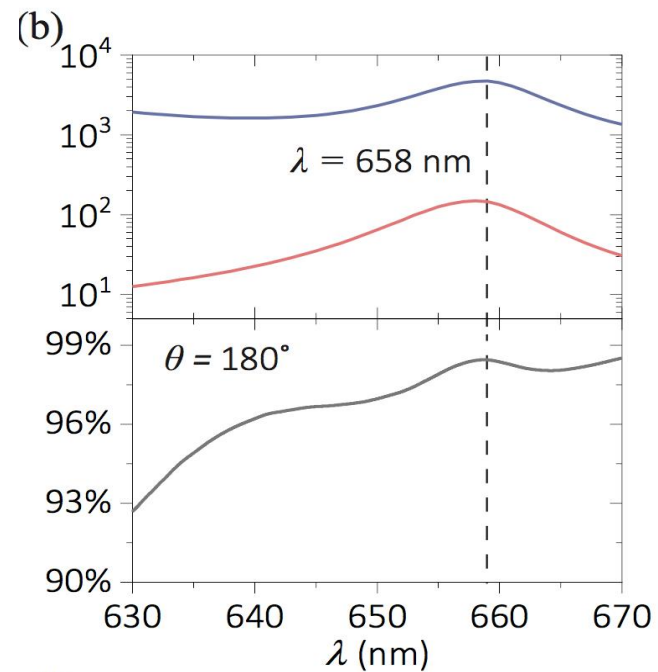
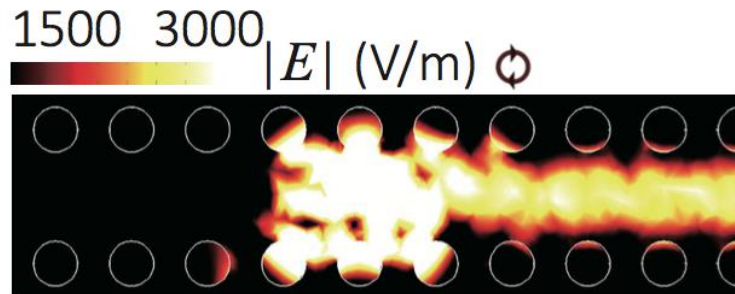
Nanoscale Direction-locked Purcell enhancement

$\gamma_{\text{tot}}/\gamma_0$ **4500 ~ 4800**

$\gamma_{\text{WG}}/\gamma_0$ **100 ~ 260**

Directionality: **93% ~ 98%**

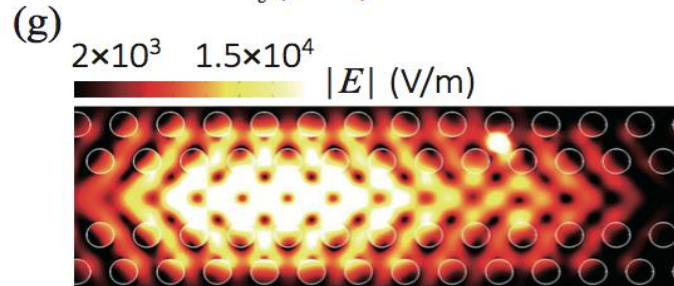
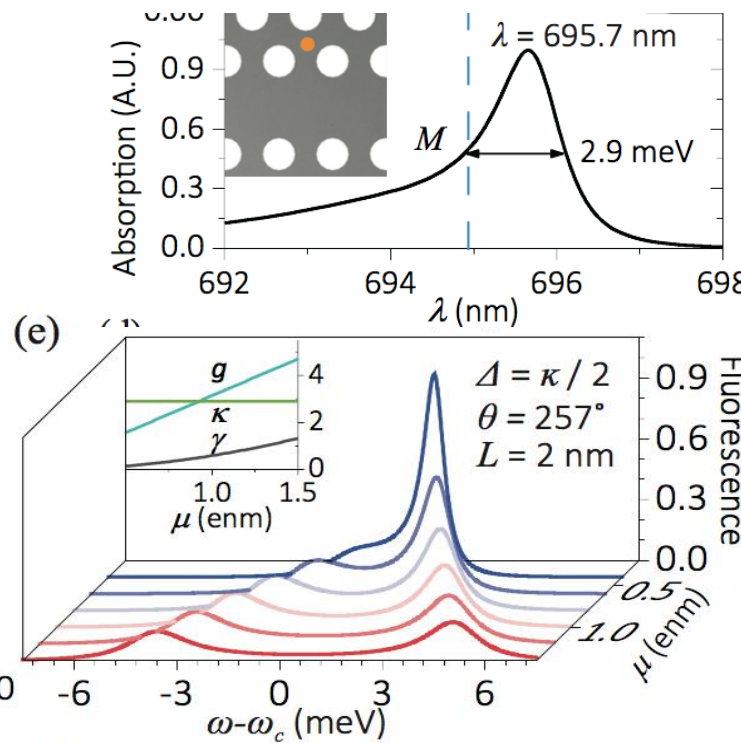
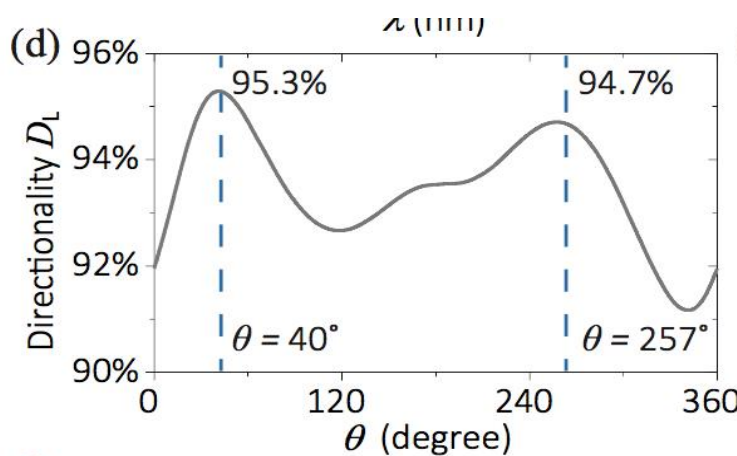
$$D_{\text{R/L}} = \frac{W_{\text{R/L}}}{W_{\text{R}}+W_{\text{L}}}$$



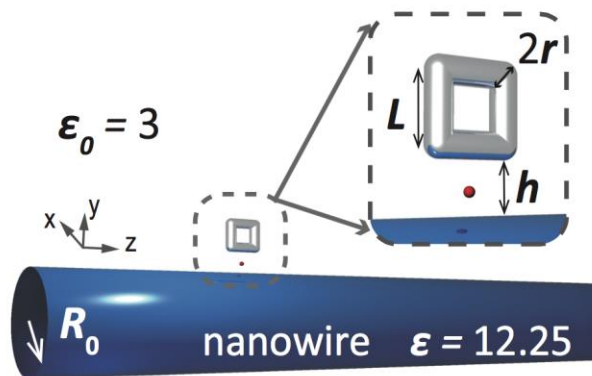
Direction-locked vacuum Rabi splitting at the nanoscale

Directionality:

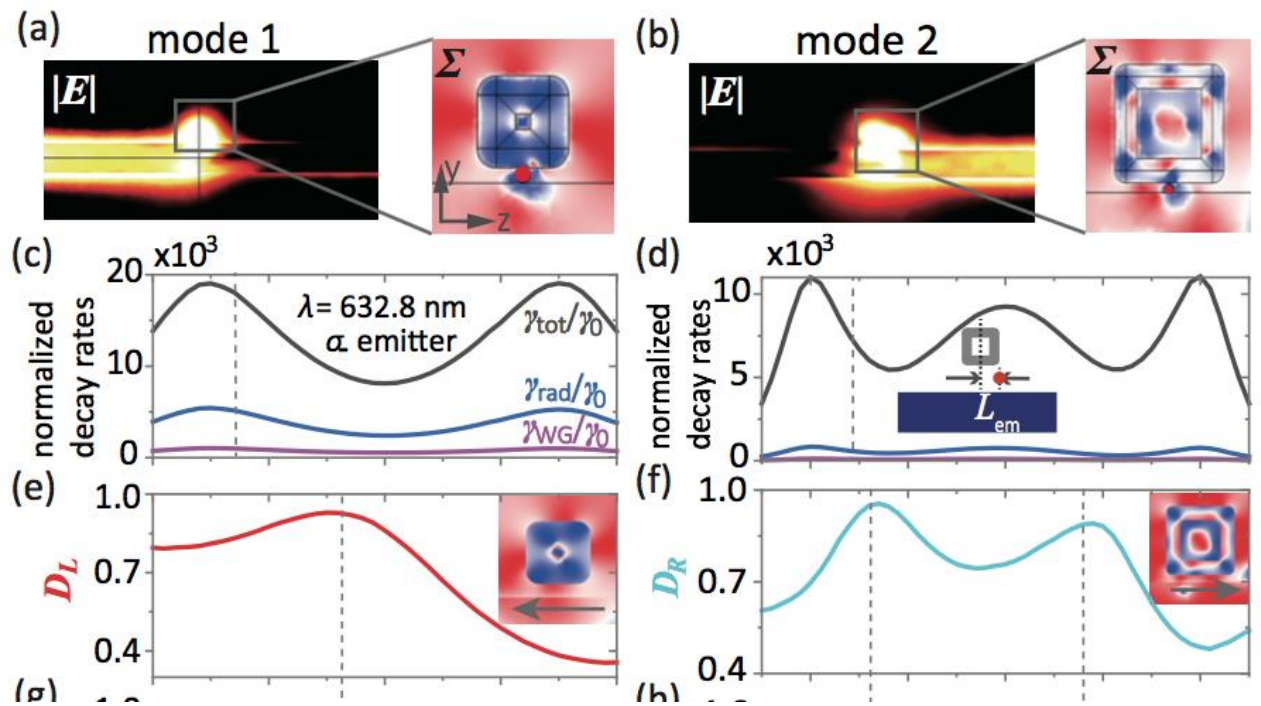
93% ~ 98%



Purcell enhancement and directional propagation control in hybrid nanowire-AgNP structure



Lingxiao Shan, Fan Zhang and Ying Gu et al. OE, Vol. 28, No. 23 / 9, 33890 (2020) 33890.

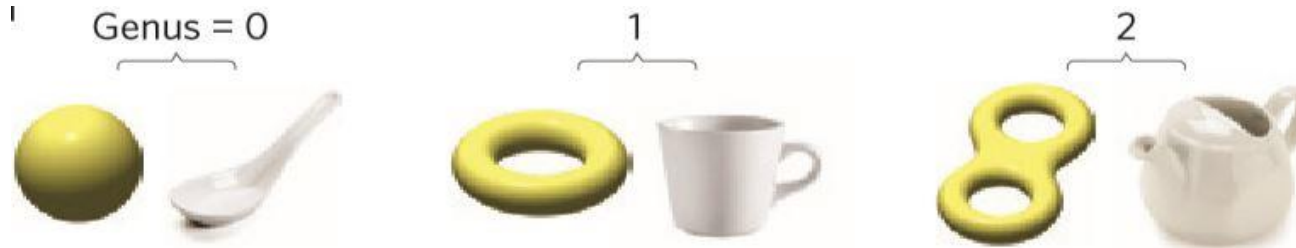


二、拓扑保护下珀塞尔效应

拓扑光子学简介

Topology grew out of the study of geometry.

Topological equivalence: reshape without cuts and glues



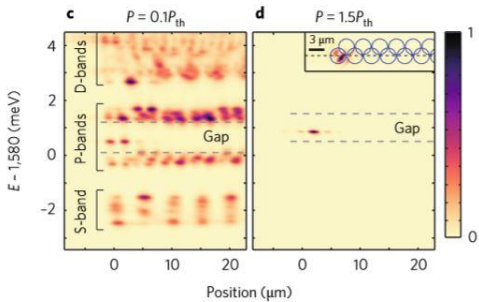
Gauge theories (1970s): topology of quantum field theory

Integer quantum Hall effect (1980s): link between geometry phase and topology, topological insulators

Nowadays: photonic system, electronic system, mechanical systems

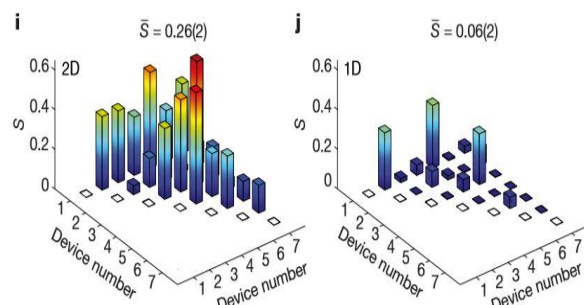
Property of topological photonics

1. Topological robustness, protection
2. Unidirectional waveguides that allow light to flow around large imperfections without back-reflection (Like Highway)
3. Bulk-edge correspondence (band&edge, no bulk no edge)



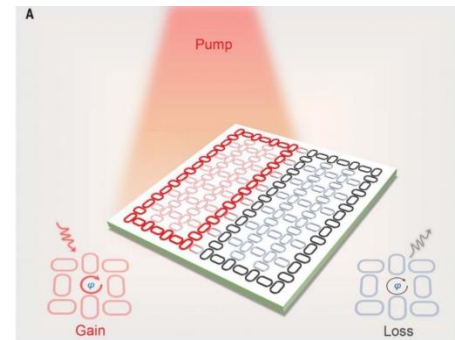
Laser

Nat.Photon. 11, 651 (2017)



Quantum light source

Nature 561, 502–506 (2018)



Non-Hermitian
light steering

Science 365.6458 (2019)

为什么做这个问题？

问题：拓扑保护下的单光子源

单光子源的角度：

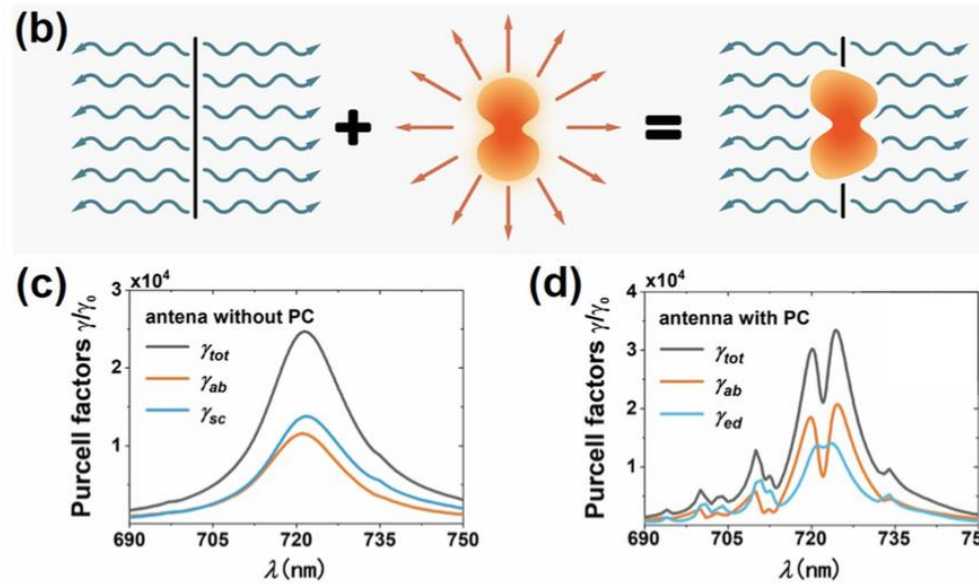
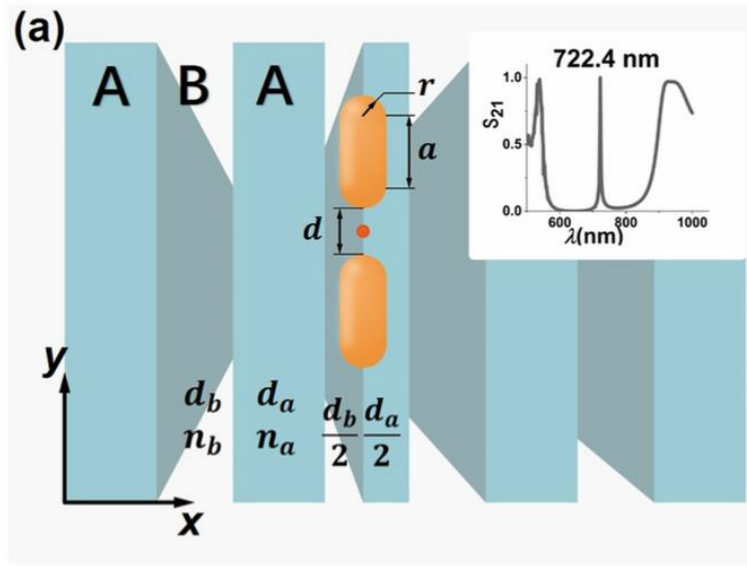
Micro/Nanoscale single photon source is an indispensable building block in on-chip quantum information processing. However, their **scattering** and **absorption** are two barriers when guiding these single photons into other devices.

拓扑的角度：

Topological states are characterized as nonscattering propagation of photons and immunity to a wide class of impurities and defects. However, introducing topological protection into the Purcell enhancement has not been reported yet.

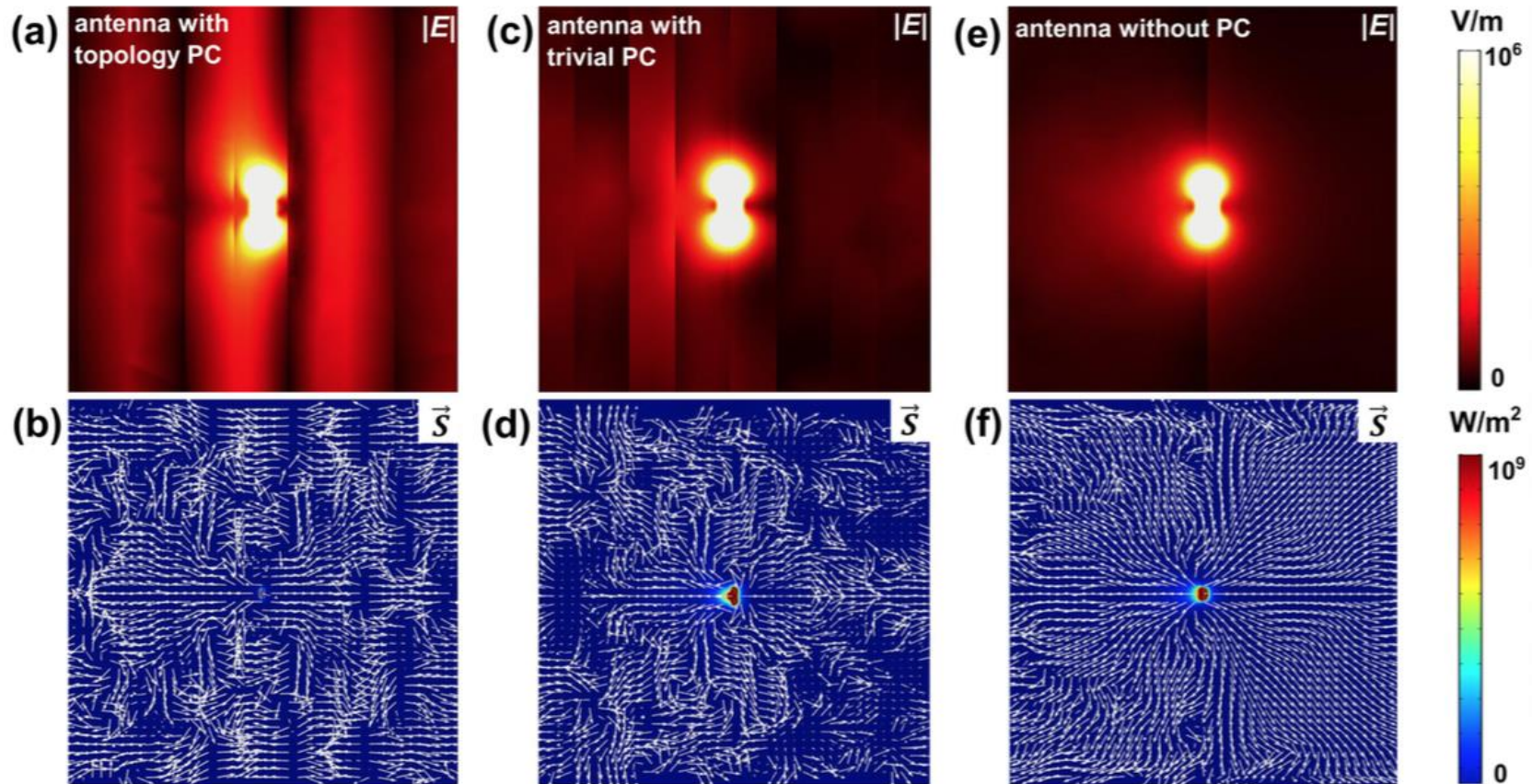
Zhiyuan Qian, Zhichao Li, and Ying Gu et al. PHYSICAL REVIEW LETTERS
126, 023901 (2021)

拓扑保护下，边界态主导的模式耦合原理



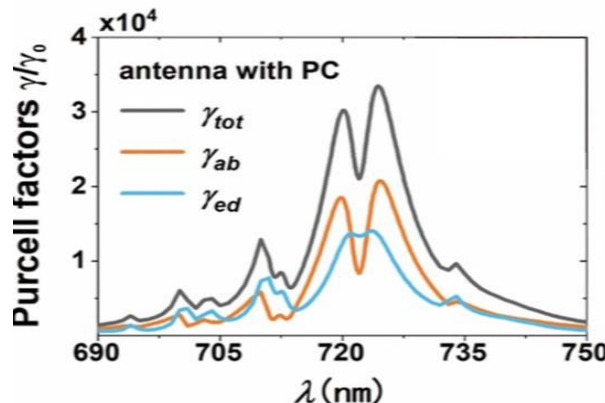
Zhiyuan Qian, Zhichao Li, and Ying Gu et al. PHYSICAL REVIEW LETTERS
126, 023901 (2021)

有无拓扑保护下电场和能流分布

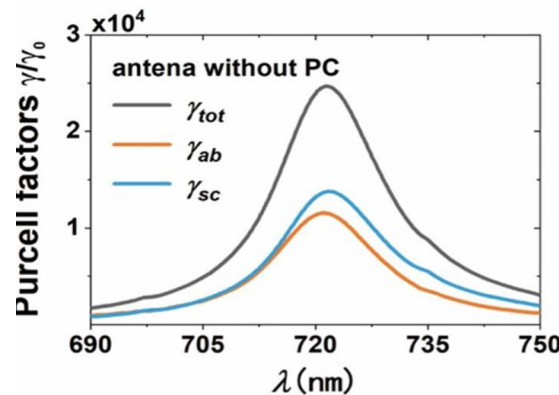


Zhiyuan Qian, Zhichao Li, and Ying Gu et al. PHYSICAL REVIEW LETTERS
126, 023901 (2021)

拓扑保护下珀塞尔系数的吸收减少



(a) Antenna with PC



(b) Antenna without PC

r (nm)	γ_{tot}/γ_0	γ_{ab}/γ_{tot}	γ_{ed}/γ_{tot}	η
5	39003	63. 2% (24659)	36. 8% (14344)	6. 857
7	22003	37. 8% (8323)	62. 2% (13680)	8. 932
10	9901	20. 5% (2029)	79. 5% (7872)	9. 725

(b) Antenna without PC

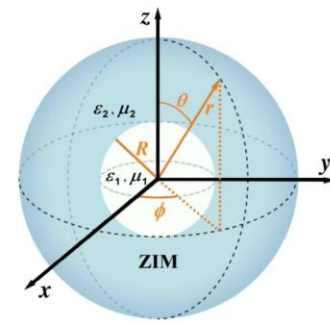
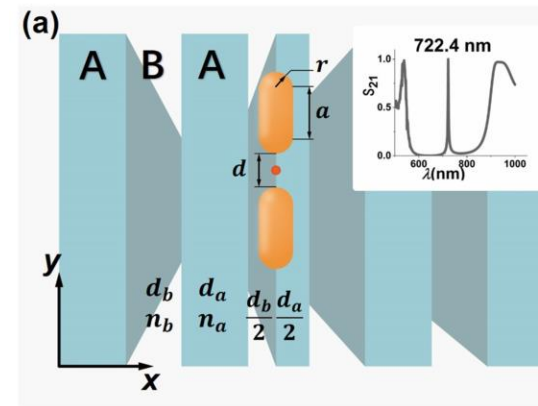
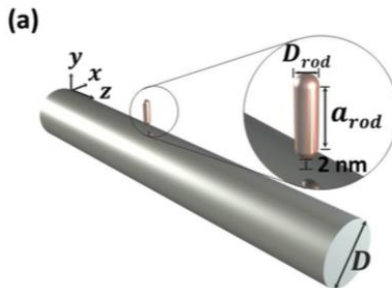
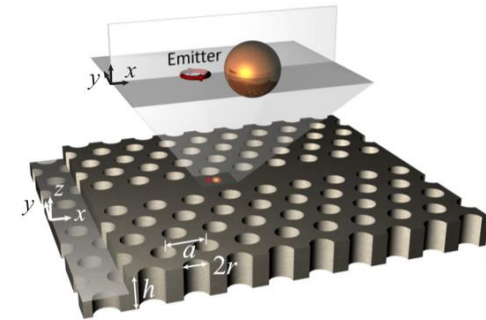
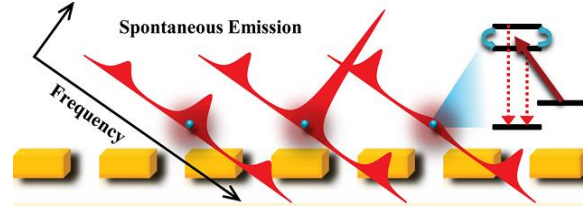
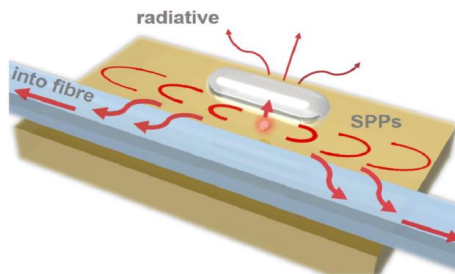
r (nm)	γ_{tot}/γ_0	γ_{ab}/γ_{tot}	γ_{sc}/γ_{tot}
5	41590	67. 9% (28252)	32. 1% (13338)
7	25298	45. 6% (11533)	54. 4% (13765)
10	12156	24. 5% (2974)	75. 5% (9182)

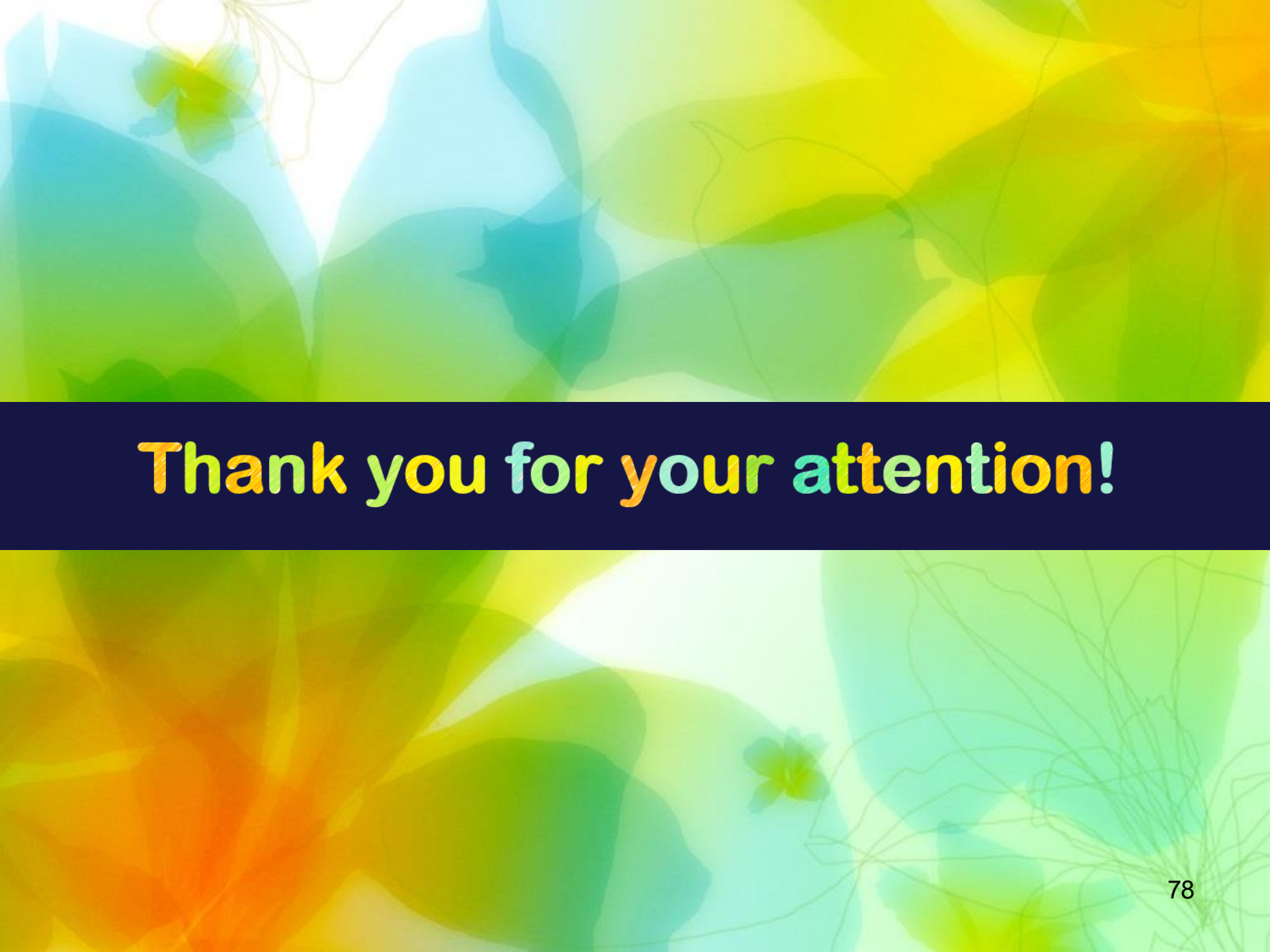
意义和展望

1. 拓扑保护性第一次用于CQED
2. 这个想法可以推广到2D或高阶拓扑结构
3. 推进拓扑结构用于单光子源和纳米激光
4. 强耦合中。 . .

总之：

研究多种微纳结构及其组合
其中的量子光场及其和量子体系耦合
腔量子电动力学、量子干涉及量子信息





Thank you for your attention!